https://doi.org/10.5194/egusphere-2024-2571
Preprint. Discussion started: 18 September 2024

Bio-climatic factors drive spectral vegetation changes in Greenland

Tiago Silva[1,2], Brandon Samuel Whitley[3], Elisabeth Machteld Biersma[3], Jakob Abermann[1,2], Katrine Raundrup[4], Natasha de Vere[3], Toke Thomas Høye[5,6], and Wolfgang Schöner[1,2]

[1]Geography and Regional Science Institute, University of Graz, Graz, Austria
[2]Austrian Polar Research Institute, Vienna, Austria
[3]Natural History Museum of Denmark, University of Copenhagen, Copenhagen, Denmark
[4]Department of Environment and Minerals, Greenland Institute of Natural Resources, Nuuk, Greenland
[5]Department of Ecoscience, University of Aarhus, Aarhus, Denmark
[6]Arctic Research Centre, University of Aarhus, Aarhus, Denmark

Correspondence: Tiago Silva (tiago.ferreira-da-silva@uni-graz.at)

Abstract.

The terrestrial Greenland ecosystem (ice-free area) has undergone significant changes over the past decades, affecting biodiversity. Changes in air-temperature and precipitation have modified the duration and conditions of snowpack during the cold season, altering ecosystem interactions and functioning. In this study, we statistically aggregated the Copernicus Arctic regional reanalysis (CARRA) and remotely-sensed spectral vegetation data from 1991 to 2023 by using principal component analysis (PCA), in order to I. examine key sub-surface and above-surface bio-climatic factors influencing ecological and phenological processes preceding and during the thermal growing season in tundra ecosystems; II. interpret spatio-temporal interactions among bio-climatic factors on vegetation across Greenland; III. investigate bio-climatic changes dependent on location and elevation in Greenland; IV. identify regions of ongoing changes in vegetation distribution.

Consistent with other studies, PCA effectively clustered bio-climatic indicators that co-vary with summer spectral vegetation, demonstrating the potential of CARRA for biogeographic studies. The duration of the thermal growing season (GrowDays) emerged as the pivotal factor across all ecoregions (with increases up to 10 days per decade), interacting with other bio-climatic indicators to promote vegetation growth. Regions with significant snow height decrease occur along with an earlier snowmelt period (up to 20 days per decade), which triggers the onset of GrowDays earlier. In most regions, we find that shallower snowpacks tend to melt slower. We hypothesise that slow snowmelt rates foster microbial activity, enriching the soil with nutrients. The combined effect of soil nutrients and the resulting warming in spring (up to 1.5°C per decade), promotes early plant development. These bio-climatic changes, in the cold and summer season, have led to northward and upward vegetation expansion. The distribution of vegetation has expanded in Northeast Greenland by 22.5% increase with respect to 2008-2023, leading to new vegetated areas. We report little to no change in the length and onset of the GrowDays along the coast in Northeast Greenland, in contrast with more pronounced changes inland and at higher elevations, hence showing an elevation-dependent response (increases up to 5 days per decade per km elevation). Our study determines a set of bio-climatic indicators relevant for understanding vegetation. These insights provide a basis to validate bio-climatic indicators from climate models to assess future vegetation changes across Greenland under a changing climate.

https://doi.org/10.5194/egusphere-2024-2571
Preprint. Discussion started: 18 September 2024

1 Introduction

The changing climate in the past decades has profound and rapid effects on Arctic ecosystems, with regional Greenland warming at nearly three times the global average (Rantanen et al., 2022). This rapid warming is causing significant changes in the region's climate patterns and ecosystems. Jansen et al. (2020) highlight that the current era of abrupt climate change in the Arctic is unprecedented in the context of the past several thousand years, leading to complex and varied responses in Arctic vegetation. Myers-Smith et al. (2020) reveal the intricacies of the "Arctic greening", where increased temperatures and earlier snowmelt drive changes in plant growth and species distribution. These changes affect ecological interactions, such as shifts in plant community composition, alterations in soil nutrient cycling, leading to feedback mechanisms involving snow cover and surface albedo. Similarly, Huang et al. (2017) discuss the rate of change in vegetation productivity across northern high latitudes, reiterating that the response to climate change is influenced by multiple factors, including soil moisture availability, temperature variations, and the timing and extent of snowmelt.

Over the last three decades, community plant height has increased across the Arctic (Metcalfe et al., 2018). This has largely been caused by plant community changes, in particular due to an increase in abundance and productivity of deciduous shrub species – causing "shrubification" of the tundra (Sturm et al., 2001). A large-scale study on the interconnection between temperature, moisture, and various key plant functional traits at 117 Arctic locations over 30 years of warming revealed a strong relationship between temperature and particular plant traits; however, soil moisture was a strong factor determining the strength and direction of these relationships (Metcalfe et al. 2018). Changes in plant communities and the expansion of deciduous shrubs with warmer summers are likely reliant on the availability of soil moisture (e.g., Ackerman et al. 2017; Gamm et al. 2018; Power et al. 2024), exhibiting a rapid rise in deciduous shrubs in wet regions, but a decline in dry tundra zones.

Due to high latitude and continentality, summer soil moisture availability is particularly important in certain areas of Greenland that are already drier than other parts. In these drier areas, higher temperatures and less precipitation during the summer can potentially cause desiccation and salt accumulation at the soil surface, with a negative effect on plant growth (Zwolicki et al., 2020). Therefore, it is expected that an increase in temperature will unlikely lead to a striking increase in plant growth, mainly due to the lack of precipitation. For instance, a study on growth responses of two widespread and dominant deciduous shrub species (*Salix glauca* and *Betula nana*) in western Greenland, using dendrochronology, stable isotope analysis, and leaf gas exchange measurements revealed that both species have declined in growth since the 1990s, likely due to increasing water limitation (Gamm et al., 2018). However, increasing herbivory also plays a role, such as increased moth outbreaks (Post and Pedersen, 2008), a growing muskoxen population in West (Eikelenboom et al., 2021) and East Greenland (Schmidt et al., 2015) and increases in geese populations in East Greenland (Boertmann et al., 2015). Such studies are however based on small-scale analysis and in contrast with observations of increasing shrub growth in other parts of the Arctic (Metcalfe et al., 2018). Also, certain inland parts of Greenland are warmer and drier than most other areas of the Arctic, and will therefore respond differently to climate change. Therefore, their spatial representativeness is unclear. The critical influence of soil water availability on future changes in tundra plant communities in Greenland should not be underestimated, and may also serve as an indicator for other drier Arctic regions, which may experience similar changes in temperature and precipitation. Additionally, while certain

https://doi.org/10.5194/egusphere-2024-2571
Preprint. Discussion started: 18 September 2024

plant communities such as the evergreen dwarf shrubs are generally better adapted to drier conditions, and have been observed to have increased with recent warming in the colder and drier High Arctic (Weijers et al., 2017), it is likely that these species also become decreasingly temperature- and increasingly soil moisture-dependent during summer (Weijers, 2022).

Temperature, precipitation, as well as water availability during the growing season are a few of the climatic indicators contributing to vegetation changes. However, other climatic indicators, such as snowfall, snow cover melt and frost also play an important role even before the onset of the growing season (Cooper, 2014). The projected warmer temperatures for the cold season will likely have a very different effect than during the growing season (Weijers, 2022). Increased snow during the cold season usually means increased growth in the following summer, as more snow provides insulation, less frost damage and an increase in water availability in the spring (e.g., Lamichhane 2021; Wang et al. 2024). Also, increased insulation has been shown to lead to an increased microbial breakdown of leaf litter and therefore an enhanced nutrient supply in the following growing season (e.g., Cooper 2014; Pedron et al. 2023). However, if snow is limited and precipitation is falling as rain rather than snow, the resulting ice conditions can have damaging effects on the vegetation (increased branch mortality and vegetation damage, Weijers 2022) and in soil nutrient cycling. Additionally, in exceptional years like 2018, the High Arctic experienced unusually large amounts of snow coverage, resulting in extraordinarily delayed snowmelt. This made it very difficult for plants to grow and for animals to access resources (Schmidt et al., 2019). Such conditions will strongly influence the growth of plants, and have impacts throughout the food chain, such as for the Svalbard reindeer (Le Moullec et al., 2020) and the caribou in West Greenland (Eikelenboom et al., 2021). Overall, the amount of snow and the coupling with temperature are highly important for plant growth, and plant community composition in the Arctic, and a Greenland-focused study assessing bio-climatic changes has not yet been made. Grimes et al. (2024) has recently shown that the doubling of vegetation across ice-free Greenland is linked with warming. However, how warming impacts other interlinked bio-climatic indicators requires further investigation.

In order to properly assess changes in bio-climatic indicators in Greenland, it is important to consider that soil water sources in the region are mainly from precipitation, snowmelt and permafrost thaw. The combination of hard local geology with scouring by the ice sheet has shaped the landscape, and thin soils result in less prevalent thermokarst and low water retention (Anderson 2020). This means that meltwater flows rather freely according to the surface gradient, eventually gathering in low-lying areas to form lakes or drains towards the sea. Therefore, tundra vegetation develops in regions adjacent to such water bodies, eventually colonizing recently drained regions (e.g., Chen et al. 2023). Due to climate warming, not only surface, but also subsurface runoff has increased in the Arctic (Rawlins and Karmalkar 2024). The increased runoff in combination with the climate–induced terrestrial greening has led to a decline in nutrients export via rivers to the sea, which decreased phytoplankton biomass in the coastal ecosystems (Søgaard et al., 2023). Given the heterogeneity in soil properties and water availability sources, sub-surface bio-climatic indicators, such as volumetric soil water and, potentially, sub-surface runoff, should be considered.

In this study, we analyse 32 years (1991–2023) of remotely-sensed Normalized Difference Vegetation Index (NDVI) data to gain a deeper understanding of the spatio-temporal patterns of spectral vegetation changes across ice-free regions of Greenland, extending beyond the representativeness of point-scale studies. Furthermore, we examine the combined effects of bio-climatic indicators ranging from sub-surface factors (such as soil water availability) to above-surface factors (such as the thermal grow-

https://doi.org/10.5194/egusphere-2024-2571
Preprint. Discussion started: 18 September 2024

ing season, heat stress, and frost) with summer spectral greenness. We also extend our study of bio-climatic changes beyond the summer by including indicators from the preceding winter and spring, assessing their combined impact with summer spectral greenness. Additionally, we explore historical trends of bio-climatic indicators individually, investigating their latitudinal and altitudinal sensitivity. Finally, we identify regions with changes in spectral greenness and in greenness distribution.

2 Data

2.1 Copernicus Arctic regional reanalysis

The Copernicus Arctic regional reanalysis (CARRA) system predominantly relies on the non-hydrostatic numerical weather prediction model HARMONIE-AROME (Bengtsson et al., 2017), laterally forced by ERA5. CARRA, with a spatial resolution of 2.5 km, assimilates the same observation datasets as ERA5 (Hersbach et al., 2020), supplemented by additional station data from the national meteorological services involved within the CARRA domain. This study employed the CARRA-West domain, which encompasses ice-free Greenland. For the ice-free Greenland domain, the additional station data that CARRA assimilates is sourced from the Danish Meteorological Institute and Asiaq-Greenland Survey networks. However, snow depth observations are not provided and not assimilated by CARRA. According to CARRA Full System documentation (Schyberg et al., 2020), ice cover extent remains constant throughout the entire reanalysis period (1991-2023). The Leaf Area Index (LAI) climatology in CARRA is updated based on the multi-year mean values from the Moderate Resolution Imaging Spectroradiometer (MODIS) MCD15A2H C6 (Yang et al. 2006; Yuan et al. 2011), and these have been used to update the ECOCLIMAP cover types for Greenland. ECOCLIMAP-I (Masson et al., 2003) is a global database utilized to initialize the soil–vegetation–atmosphere transfer schemes within CARRA. Soil properties in CARRA are derived from the Harmonized World Soil Database (Nachtergaele et al., 2010). The CryoClim project has generated a satellite-derived product of snow extent, which provides access to data collected on a daily basis from 1982 to 2015. CryoClim is a worldwide, optical snow product that utilizes the historical Advanced Very High-Resolution Radiometer - Global Area Coverage (AVHRR GAC) data (Stengel et al. 2020). In the context of CARRA, the CryoClim data is ultimately chosen due to its comprehensive coverage for the entire period up to 2015.

The derived precipitation from CARRA was taken from its underlying model forecast system and is not an assimilated product. Hence, to minimize the impact of the spin up, we followed the CARRA Full System documentation (Schyberg et al., 2020), which suggests combining 12 h accumulated precipitation by the difference of precipitation at lead time 18 and 6 h from forecasts initiated at 00 UTC and 12 UTC. This procedure was used for determining liquid precipitation (time integral of rain flux) and total solid precipitation (time integral of total solid precipitation flux).

2.2 NOAA Climate Data Record for Normalized Difference Vegetation Index

Phenology studies in remote sensing utilize data collected by satellite sensors, which determine the spectrum of light absorbed and reflected by majorly green vegetation. Specific pigments present in plant leaves exhibit a pronounced absorption of visible

https://doi.org/10.5194/egusphere-2024-2571
Preprint. Discussion started: 18 September 2024

light wavelengths, particularly those in the red spectrum. Conversely, the leaves exhibit a strong reflection of near-infrared light wavelengths. While numerous vegetation indices exist, one of the most prevalent is the Normalized Difference Vegetation Index (NDVI), which uses red and near-infrared bands. NDVI serves as a measure of spectral vegetation health and spans from -1 to 1.

The National Oceanic and Atmospheric Administration (NOAA) Climate Data Record (CDR) using the AVHRR (Vermote et al. 2018) NDVI, Version 5 (hereafter AVHRR NDVI) and NOAA CDR using the Visible Infrared Imager Radiometer Suite (VIIRS, Vermote et al. 2022) NDVI, Version 1 (hereafter VIIRS NDVI) are jointly used in this study from 1991 to 2023 on a daily basis with 0.05 degrees grid resolution (approx. 5.5 km in latitude and around 2.5 and 0.5 km between 60 and 85 degrees North, respectively). AVHRR NDVI is available until the end of 2013, and thereafter is then continued by its successor VIIRS NDVI. AVHRR NDVI uses the MODIS Land-Sea mask and its cloud mask spectrally adjusted using 10 years of MODIS data, with 90% match accuracy over land (Franch et al. 2017). As VIIRS will eventually replace MODIS, MODIS is used to calibrate VIIRS NDVI estimates (Skakun et al. 2018).

As both gridded products in this study have different spatial resolutions, spectral greenness from NOAA NDVI is spatially interpolated to the CARRA grid with resolution of 2.5 km.

3 Methods

3.1 Spectral greenness

Arctic regions are characterized by sparse vegetation, that typically exhibit markedly low NDVI values, often as low as 0.15, with dense shrubs above 0.5, and signal saturation at around 0.7 (e.g., Myers-Smith et al. 2020; Liu et al. 2024; Walker et al. 2005). Based on the daily datasets provided by AVHRR NDVI and VIIRS NDVI, monthly (averaged) NDVI (monthly NDVI $= \frac{\sum_{n=1}^{n} \mathrm{NDVI}_i}{n}$, where n is the total number of observations in a month) is calculated pixel-wise for days with NDVI$\geq$0.15. Estimates integrated through time are less likely to be influenced by temporal sampling artefacts at high latitudes than metrics based on maximum NDVI (e.g., Myers-Smith et al. 2020). Pixels with monthly NDVI equal or higher than 0.15 are also used to determine the interannual extent of vegetation.

While AVHRR NDVI only raises a polar flag above 60 degrees of latitude, VIIRS NDVI applies a more strict quality control, effectively flagging not only clouds but also snow at polar latitudes. Consequently, n is higher for AVHRR NDVI than for VIIRS NDVI, impacting monthly NDVI for AVHRR NDVI. As pixels with snow-cover, clouds and shadow are not flagged in AVHRR NDVI, that certainly influenced surface reflectance, we used the monthly minimum, mean and maximum of n from VIIRS for each year between 2014 and 2023 to estimate monthly uncertainty in spectral greenness between 1991 and 2013. In this way, we assume similar occurrence of pixels with snow-cover, clouds and shadow throughout the study period. Figure S1 presents the monthly spatial extent (number of observations multiplied by area) recorded by AVHRR and VIIRS from 1991 to 2023 across all ecoregions to ensure comparable interannual spatial coverage. Finally, we calculated a seasonally averaged NDVI, hereafter referred to as spectral greenness and interchangeably as vegetation.

https://doi.org/10.5194/egusphere-2024-2571
Preprint. Discussion started: 18 September 2024

3.2 Bio-climatic factors

The set of chosen bio-climatic indicators were inspired by previous work from Aalto et al. (2023) and Rantanen et al. (2023), who proposed and investigated bioclimatic indices in Finland and across the Arctic. Our study emphasizes Greenland, considering adapted thresholds and additional climatic factors.

Table 1. Brief description of the bio-climatic indicators derived in the study.

Bio-climatic Indicator	Description	Units
T_{2m}	seasonally averaged air-temperature at the height of 2 m above the surface	°C
SWE_{MAX}	mass of liquid water from melting the snow per unit area	mm w.e.
SWE_{MAX}DOY	day of the year for SWE_{MAX}	day of the year
SnowDays	snow-covered days when SWE is higher than 10 mm w.e.	days
GrowDays	days with daily T_{2m} higher than 1 °C that does not belong to SnowDays	days
DegreeDays	sum of daily T_{2m} during GrowDays	K days
Onset	first day of GrowDays	day of the year
End	last day of GrowDays	day of the year
MeltRate	fraction of SWE_{MAX} by the number of days between SWE_{MAX}DOY and Onset of GrowDays	mm w.e. day^{-1}
(Spectral) Greenness	seasonally averaged monthly NDVI, as described in Section 3.1	unitless
Snow	seasonally accumulated mass per unit area of snow and ice particles falling on the surface	mm w.e.
RainRatio	fraction of liquid precipitation of the total precipitation	%
RainOnSnow	RainRatio higher than 50% in SnowDays	days
VPd	vapour pressure deficit is the difference between the amount of water vapour in the air and the amount of water vapour the air can hold when it is saturated	hPa
VSI	seasonally averaged water equivalent of volumetric soil ice content	%
VSW	seasonally averaged volumetric liquid water in the soil	%
FrostDays	SWE lower than 10 mm w.e. in spring with negative daily T_{2m}	days
DroughtDays	days with precipitation lower than 1 mm w.e. lasting for more than 10 consecutive days	days
HeatDays	days exceeding the seasonal T_{2m} climatology for the period 1991-2023 by 2 SD	days
Longitude	distance east or west of the Greenwich meridian	degrees
Latitude	distance north of the equator	degrees
Elevation	vertical elevation above sea level	m a.s.l.

From CARRA daily-averaged snow water equivalent (SWE), we derived the maximum SWE (SWE_{MAX}), the day of the year SWE_{MAX} occurs (SWE_{MAX} DOY) and snow-covered days (SnowDays) when SWE > 10 mm of water equivalent (w.e.). It is

https://doi.org/10.5194/egusphere-2024-2571
Preprint. Discussion started: 18 September 2024

important to note that SnowDays are not necessarily continuous, with sporadic snow events occurring all year-round. van der Schot et al. (2024) provides a thorough validation of CARRA SWE with in situ observations across Greenland. They report that CARRA is capable of successfully representing snow-related indicators such SWE_{MAX} and SWE_{MAX} DOY.

We calculated GrowDays by considering days that do not belong to SnowDays, with daily-averaged 2 m air-temperature (T_{2m}) > 1 °C. The onset (i.e. the first) and termination (i.e. the last) day of the year of GrowDays are also derived. The indicator DegreeDays is obtained by summing up T_{2m} during the previously defined GrowDays. The daily rain ratio (RainRatio) is defined as the fraction of liquid precipitation of the total precipitation. SnowDays, in combination with RainRatio higher than 50%, are used to derive days with rain-on-snow (RainOnSnow) between January and September. SWE_{MAX} DOY and thermal growing season onset are used to determine the length of the snow melting period (SWEmeltDays). Dividing SWE_{MAX} by SWEmeltDays, we estimate the averaged snow melting rate (MeltRate).

Certain bio-climatic indicators used in this study are based on seasonal statistics using the definition of meteorological seasons: winter includes December to February (DJF), spring from March to May (MAM), summer from June to August (JJA) and autumn from September to November (SON). Spectral greenness, T_{2m}, RainRatio, the volumetric soil water and ice (SoilWater and SoilIce) and vapour pressure deficit (VPd) are seasonally averaged, whereas precipitation, snowfall (Snow) and rainfall (Rain) are seasonally accumulated.

The vapour pressure deficit in summer (VPdJJA), which is the difference between the water vapour pressure of saturated air and the actual water vapour pressure in the air, was calculated to represent continentality. Continentality in summer is expressed by high temperatures and lower humidity due to large distances to moisture sources. This lack of moisture availability contributes to lower water vapour pressure, which, when combined with high temperatures, leads to higher VPd. A high VPdJJA indicates a strong drying potential in the atmosphere, which can significantly influence evaporation rates and plant water stress (e.g., Grossiord et al. 2020; Yuan et al. 2019).

DroughtDays, the number of days with precipitation lower than 1 mm w.e. lasting for more than 10 consecutive days, is seasonally aggregated in spring and summer. HeatDays are also seasonally aggregated in spring and summer, and they consist of the number of days exceeding the seasonal T_{2m} climatology for the period 1991-2023 by two standard deviations (2SD). As the 32-year period is fairly normal distributed, +2SD are approximately equivalent to 97.5th percentile. FrostDays in spring are derived in the absence of snow cover, jointly with negative T_{2m} days.

Spectral greenness was narrowed to summer, in order to capture the period with maximum solar radiation in Greenland and avoid snow-covered patches. Given the fact that shadow areas heavily impact reflectance, latitudes higher than 75°N are not considered due to low sun elevation. We restrict our study area to West and Northeast Greenland, as steep mountains, deep fjords, expansive glaciers, and extensive ice caps inhibit the method's applicability in Southeast Greenland.

3.3 Ecoregions

Greenland extends for approximately 23 degrees of latitude, with temperature and precipitation rates varying considerably across latitudes and coasts (Westergaard-Nielsen et al., 2020). Due to the semi-permanent Icelandic Low and the steep topography, the Southeast coast receives more precipitation than the Southwest coast (e.g., Ettema et al. 2010; Fettweis et al. 2017).

https://doi.org/10.5194/egusphere-2024-2571
Preprint. Discussion started: 18 September 2024

In general, the West and East coasts exhibit different topographic features, from a topographically complex East contrasting with predominantly glacially eroded regions in the West (e.g., Karami et al. 2017; Anderson 2020). Nevertheless, both coasts comprise diverse fjord systems, that often channel the wind and shield inland areas against storms. Consequently, the north-facing slopes and the leeward side of these inland mountain systems receive reduced precipitation. Such coast-inland gradients are therefore complex, also influencing the distribution of permafrost and freshwater systems (e.g., Westergaard-Nielsen et al. 2018; Abermann et al. 2019). Not only precipitation, but also temperature, tends to decrease with latitude. Other factors known to shape the coastal climate are prominent ocean currents (e.g., East Greenland and North Atlantic current) as well as sea ice and fjord ice conditions (e.g., Westergaard-Nielsen et al. 2020; Shahi et al. 2023).

The Arctic tundra ecosystem, including Greenland, is typically separated at around 70°N into Low Arctic and High Arctic based on climatic and vegetation differences (Bliss et al., 1973). Greenland has also been mapped according to hydrology, soil pH, percentage of water cover, floristic provinces and bioclimatic subzones (e.g., Walker et al. 2005). The former mapping partly relies on mean July temperature thresholds and positive degree month temperatures to classify subzones. However, the T_{2m} JJA has warmed at a median rate of approx. 1°C per decade since 1991 (Fig. S2), likely shaping plant community structure and distribution. Eythorsson et al. (2019) also shows that Köppen-Geiger classification and snow cover frequency in the Arctic have changed and will continue to change in the Arctic this century. In order to avoid time varying metrics, we split ice-free Greenland into five ecoregions (Fig. 1) based on physiogeographic features, such as adjacent seas, ocean currents and ice caps, with direct and indirect control on heat and moisture transport.

Ecoregion 1 is the narrow coast along the Baffin Bay in Northwest Greenland, including Sigguup Nunaa, Uummannaq fjord, Nuussuaq Peninsula and Disko Island. Disko Island is known as the transition region between High Arctic to Low Arctic, with a smooth transition of High Arctic to Low Arctic vegetation type in between ecoregions 1 and 2. Ecoregion 2 stretches from Ilulissat to the Maniitsoq Ice Cap. This ice-free part is particularly widely stretched from West to East, with climates ranging from maritime at the coast to continental in the dry interior. Ecoregion 3 encloses mainly Southwest Greenland along the Labrador Sea until Nunarsuit, curving from the Labrador Sea to the North Atlantic. The Ecoregion 4 comprises the mountainous and southernmost end of Greenland, facing the North Atlantic. Southeast Greenland, a very narrow coast composed of steep slopes, is the meeting point between the relatively cold East Greenland current and the relatively warm Irminger Current, leading to very foggy conditions during the warm season (e.g., Gilson et al. 2024; Laird et al. 2024). The combination of this region's complex topography with frequent cloud cover resulted in its exclusion from the analysis. Finally, ecoregion 5 spans from Kangertittivaq (Scoresby Sound) to the North coast of Young Sound, including Daneborg and Zackenberg. The coast of ecoregion 5 is also commonly affected by fog conditions. However, the coastal topography usually shelters inland regions. The Stauning Alps, the large system of mountain ranges west of Kangertittivaq, is excluded due to its very rugged and complex topography, with numerous rocky peaks and active glaciers in most valleys and only minor vegetation growth.

https://doi.org/10.5194/egusphere-2024-2571
Preprint. Discussion started: 18 September 2024

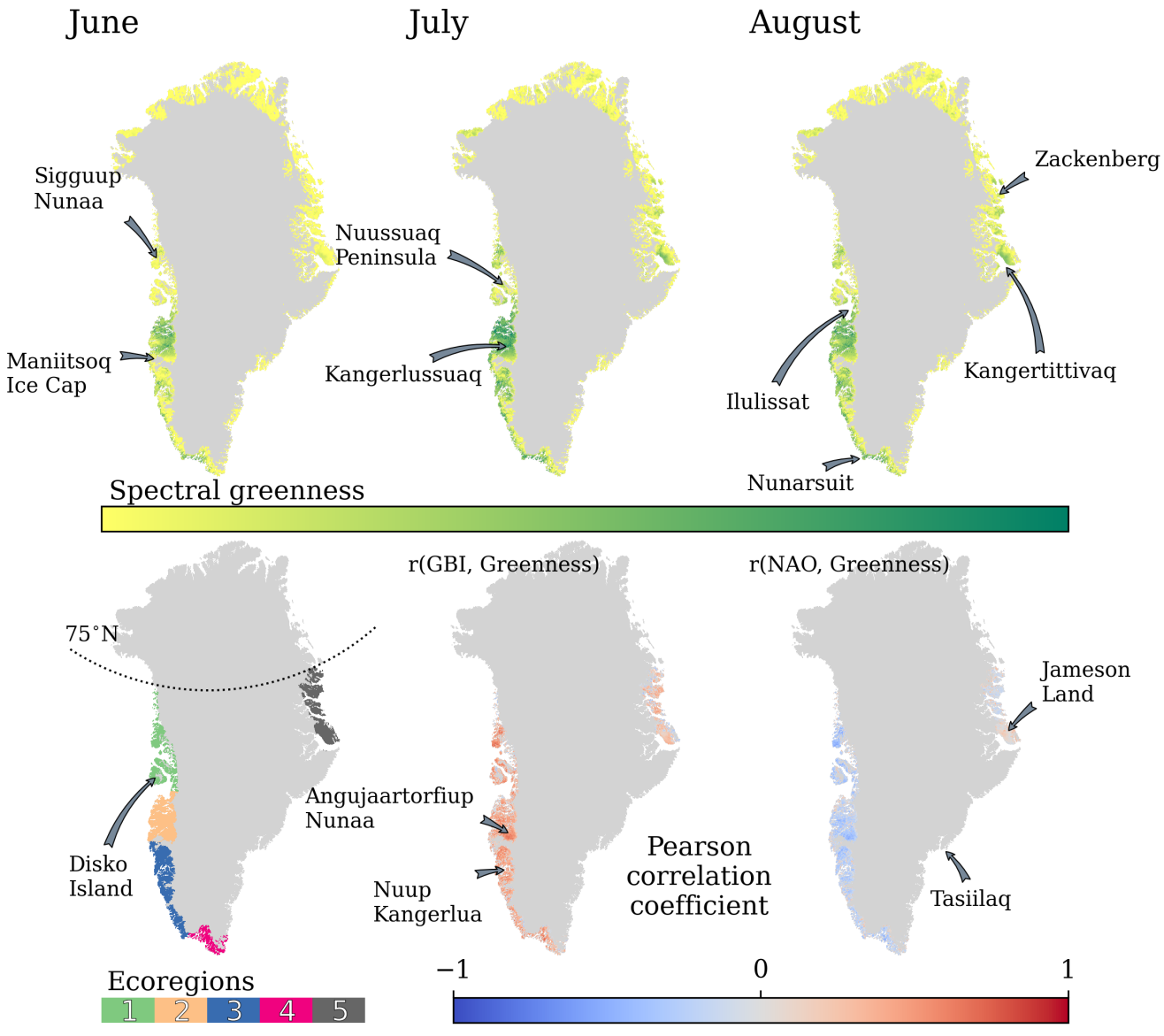

Figure 1. Averaged spectral greenness (based on the period 1991-2023) for June, July and August (upper panel). No scale shown in the colour bar because the aim is to illustrate spectral greenness patterns, not absolute values; ecoregions in ice-free Greenland (lower left panel); Pearson correlation coefficient between the summer averaged vegetation and the Greenland Blocking Index (GBI, lower central panel), and the North Atlantic Oscillation (NAO, lower right panel). Placenames referenced in the study are displayed.

The onset of the thermal growing season is inherently linked with distance to coast, elevation and latitude. While distance to coast and elevation control precipitation and snow depth, latitude controls sunlight duration and near-surface air-temperature. Due to less elevated and less topographically complex terrain, the thermal growing season starts earlier at the West (on average

https://doi.org/10.5194/egusphere-2024-2571
Preprint. Discussion started: 18 September 2024

[5thpercentile, 95thpercentile], DOY: 140 [103, 172]) than at the East Coast (DOY: 171 [145, 204]). Moreover, both latitude and elevation are crucial in cooling the atmosphere, allowing snowfall to occur, which in turn marks the end of the thermal growing season. The ecoregion with the most GrowDays is ecoregion 4 (140[76, 198] days), followed by ecoregion 2 and 3 (119 [75, 145] and 121 [77, 164] days), with less than 100 GrowDays in ecoregion 1 and 5 (97 [56, 132] and 78 [47, 108]). Due to the proximity to the Atlantic cyclone track, ecoregion 4 receives the most precipitation, accumulating to SWE_{MAX} of 432 [114, 984] mm w.e. In contrast, ecoregion 2 receives about 25% of the precipitation received by ecoregion 4, with SWE_{MAX} of 143 [64, 325] mm w.e. This is due to the fact that the interior of ecoregion 2 is surrounded by high peaks in the south (e.g., Maniitsoq Ice Cap), serving as a physical barrier for poleward moisture transport.

The correlations between Greenness and North Atlantic Oscillation (NAO) index and the Greenland Blocking Index (GBI) are shown in Figure 1. NAO and GBI are well-known climate oscillations, frequently utilized to characterize the main atmospheric circulation pattern. The NAO is determined by the surface pressure difference between the semi-permanent Subtropical (Azores) High and the semi-permanent Subpolar (Icelandic) Low (Hurrell et al., 2003), and its sign indicates the intensity of the North Atlantic jet stream. The phase of the NAO can explain most of the heat and moisture transported poleward, as well as temperature and precipitation anomalies in the periphery of Greenland (Bjørk et al., 2018). The GBI represents the average geopotential height at 500 hPa over Greenland (Hanna et al., 2016). This index reflects the prevailing atmospheric circulation pattern, quantifying the strength of heat and moisture transport over the Greenland region. Consequently, the GBI shows a strong correlation with near-surface variables in summer (e.g., Hanna et al. 2013; Hanna et al. 2015), such as spectral greenness.

3.4 Statistical methods

Principal Component Analysis (PCA) was used to investigate the combined influence among bio-climatic indicators on summer greenness changes. PCA (Pedregosa et al., 2011) operates upon several assumptions, including I. linearity, which assumes that the relationships between variables can be adequately described by linear transformations; II. that there are no significant outliers in the data; III. that there is homoscedasticity, meaning that variables have equal variance. In order to overcome heteroscedasticity, we standardized all variables for each ecoregion, centring the distribution around 0 and scaling it to a standard deviation of 1. We used quartiles and the interquartile range (IQR) to filter out values beyond the upper ($Q_3 + 3\times$IQR) and lower outer ($Q_1 - 3\times$IQR) fence, with Q_1 and Q_3 as first and third quartile, respectively. Finally, we run a PCA for a set of bio-climatic indicators in every ecoregion until at least 90% of the cumulative explained variance is reached, omitting components contributing to minimal explained variance in order to accelerate the computation process.

We used the non-parametric Mann-Kendall (M-K) trend test (Hussain and Mahmud, 2019) to assess trend monotonicity and significance among bio-climatic indicators. The trend magnitude retrieved over decadal timescales corresponds to the Theil-Sen (T-S) estimator, a robust regression method that does not require the data to be normally distributed, hence less vulnerable to outliers than conventional methods. Trends that exhibit confidence levels higher than 90 % are highlighted and treated as significant trends.

https://doi.org/10.5194/egusphere-2024-2571
Preprint. Discussion started: 18 September 2024

4 Results

The vegetation extent has progressed at different rates across summer months and ecoregions (Fig. 2). Given the colder temperatures in ecoregions 1 and 5, vegetation growth was generally not evident until July, contrasting with the more southerly located ecoregions. However, as shown below in recent years, vegetation extent was starting to increase already in June. In the southern ecoregions, the thermal growing season onset was much earlier, and some vegetation growth is seen in the spring months. This is particularly pronounced in ecoregion 2, due to the shallow snow cover. By June, the vegetation was already quite developed, reaching its maximum extent in July. Ecoregion 2 comprises the largest vegetation extent, with vegetation covering approximately 80% of its area in 2015 and 2016.

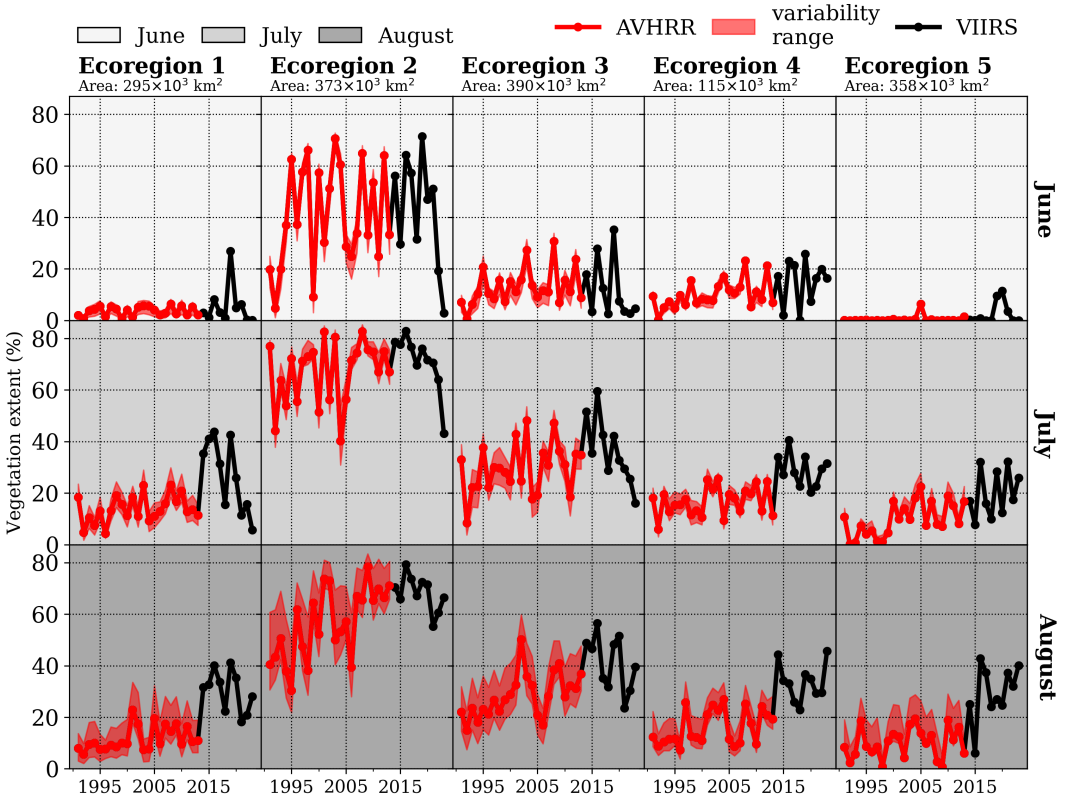

Figure 2. Development of vegetation extent between 1991 and 2023 for June (upper row), July (middle row) and August (bottom row) across ecoregions based on AVHRR (red) and VIIRS (black). The AVHRR variability range is shaded in red, given the monthly minimum and maximum number of observations within VIIRS period (2014-2023).

It should be noted that prevailing weather patterns during summer months can accelerate or delay the maximum vegetation extent (Fig. 1). Significant long-term trends in vegetation extent are not perceived, despite frequent, long-lasting and intense summer atmospheric blocking conditions in the past decades in the vicinity of Greenland.

https://doi.org/10.5194/egusphere-2024-2571
Preprint. Discussion started: 18 September 2024

4.1 Interconnectedness among bio-climatic indicators

As PCA requires the variables to be linearly related, we investigated the Pearson correlation coefficient among linearly detrended bio-climatic indicators for each ecoregion separately. The result for ecoregion 2 is shown in Fig. 3. The magnitude of the statistical links vary across ecoregions, but the direction remains generally the same. Here, bio-climatic indicators with similar correlations are sorted with hierarchical clustering, which helps to visually discern bio-climatic indicators with comparable statistical relationships.

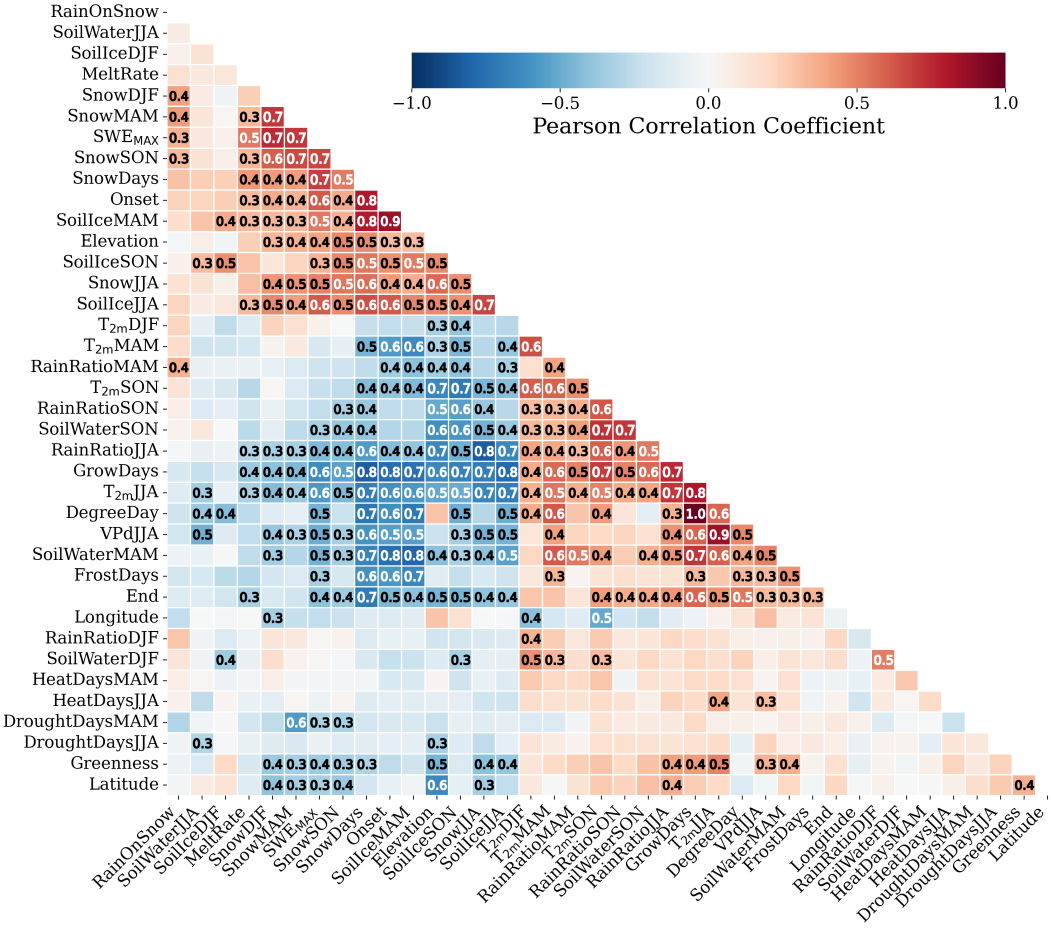

Figure 3. Correlation matrix for the bio-climatic indicators in Ecoregion 2, including Elevation, Longitude and Latitude. The correlation coefficient is colour-coded and the absolute value noted for absolute correlation coefficients higher than 0.3. The abbreviations of the bio-climatic indicators are described in Section 3.2 and in Table 1.

We investigated the correlations among all the bio-climatic indicators, including physical features like elevation, latitude and longitude. These physical features are connected to climate attributes across ecoregions. For instance, the higher the elevation

https://doi.org/10.5194/egusphere-2024-2571
Preprint. Discussion started: 18 September 2024

and latitude, the lower the precipitation rates. It should be noted that these physical features are constant through time and were not considered when investigating the combined effect among bio-climatic indicators with greenness in the PCA.

A few bio-climatic indicators, such as DroughtDaysJJA, HeatDaysMAM, HeatDaysJJA, generally show correlations lower than 0.3, except DroughtDaysMAM that significantly explains reductions in SnowMAM and partly in SWE_{MAX}. This indicates that the decrease in DroughtDaysMAM is accompanied by more frequent snowfall events, and not necessarily to more intense snowfall events. HeatDaysJJA are partly explained by T_{2m}JJA, suggesting that the increased summer air-temperature in recent years is associated with the increase of summer heat days. As greenness correlates stronger with seasonal temperatures and precipitation rates than with the above-mentioned bio-climatic indicators, and since part of their variability is explained by seasonal statistics, we excluded them from the subsequent analysis. However, it is important to highlight that the increase of Heat and DroughtDays in spring and summer are also reflected by increased air-temperatures. This is because high-pressure systems, which are typically linked with clear skies, occur more often and transport warm air from southern latitudes. RainOnSnow seems to be linked with the increase of the RainRatioMAM, but also with SnowMAM, as precipitation is likely a mix of rain and snow. It is noticeable, that RainOnSnow is increasing along East Greenland and FrostDays are locally increasing in West Greenland. However, summer spectral greenness, which is more representative of resilient plant communities, is not statistically responding to these two bio-climatic indicators. Therefore, we removed them before further analysis. The increase in FrostDays is directly linked with early disappearance of the snow-cover and partly affected by shallower snowpacks. As surface and sub-surface melt is ongoing under snow-free days, FrostDays are highly correlated with the decreasing volume of ice in the soil in spring (SoilIceMAM). SoilIce is to a large degree negatively correlated with the volume of water in the soil (SoilWater). Therefore, we decided to use SoilIce in winter (SoilIceDJF) and summer (SoilIceJJA) and SoilWater in spring (SoilWaterMAM) and autumn (SoilWaterSON) in the further analysis. Additionally, SnowDays and DegreeDays are not used since both are highly explained by GrowDays. While DegreeDays sum up T_{2m} during GrowDays, SnowDays is complementary of GrowDays, FrostDays and snow-free occasions with daily T_{2m} between 0 and 1 °C. In this way, we reduced the number of indicators that will be used as part of the PCA, diminishing "noise" and boosting the explained variance across atmosphere-biosphere-cryosphere interactions.

4.2 Bio-climatic indicators driving greenness

PCA was used to investigate the combined influence among bio-climatic indicators with summer greenness. 16 bio-climatic indicators were chosen that maximised the explained variance, whilst minimising redundant information. Figure 4 displays the combined influence of the 16 bio-climatic indicators based on the first two principal components across ecoregions. These two principal components account for most of the variability, ranging from 51% in ecoregion 2 to 65% in ecoregion 4 (Fig. S3). Due to a change of satellite sensor from 2014 onwards, we investigated how PCA performs interannually and whether there was a statistically significant change of the explained variance for years before and after 2014. The result is shown in Figure S4, displaying that the two independent samples of explained variance have identical averages in all ecoregions, with a 90% confidence level, as determined by a two-sample t-test.

https://doi.org/10.5194/egusphere-2024-2571
Preprint. Discussion started: 18 September 2024

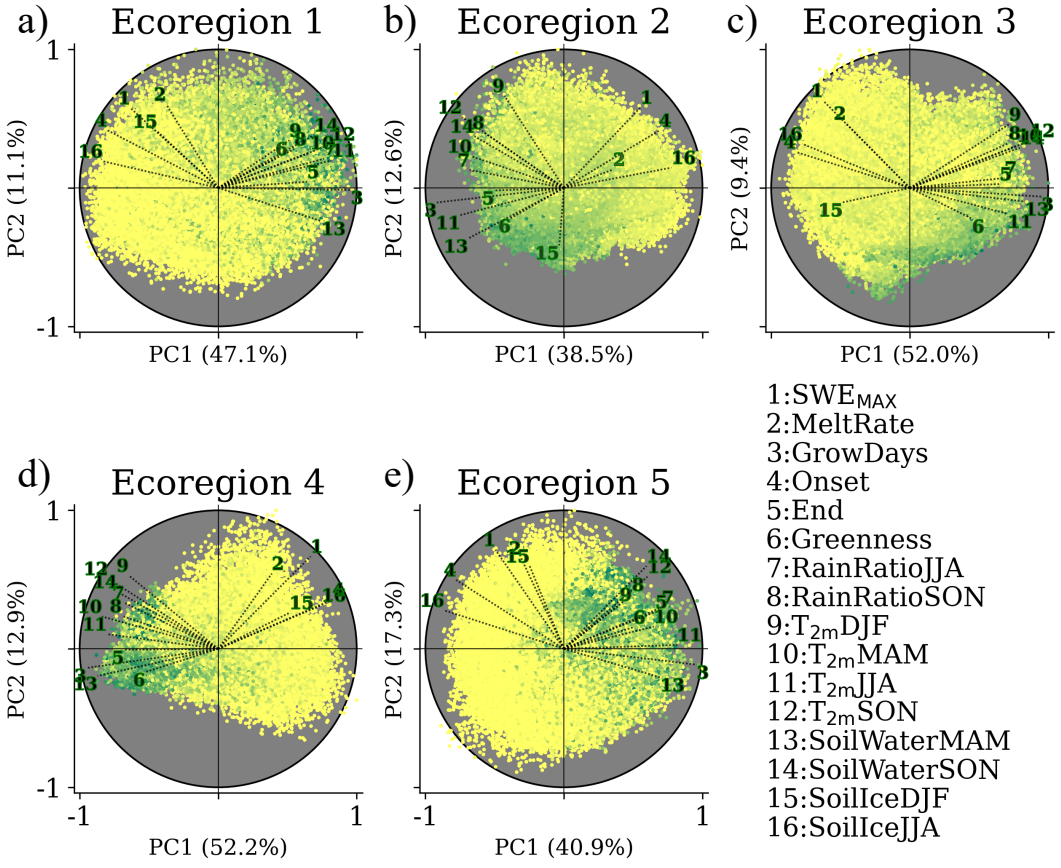

Figure 4. Biplot for scores between 1990 and 2023 for each ecoregion. The loading vectors are labelled and scaled by the maximum of each principal component. The scores are colour-coded based on the summer spectral greenness as in Figure 1, with different scales to enhance greenness. The explained variance of the first (PC1)and second (PC2) component is labelled in the corresponding axis of the subplot. The 16 bio-climatic indicators are 1: maximum snow water equivalent (SWE_{MAX}); 2: averaged snow water equivalent melt rate (MeltRate); 3: total number of thermal growing days (GrowDays); 4 and 5: start (Onset) and termination (End) of GrowDays; 6: summer spectral greenness (Greenness); 7 and 8: averaged rain ratio in summer (RainRatioJJA) and autumn (RainRatioSON); 9, 10, 11, 12: averaged 2-m air-temperature in winter (T_{2m}DJF), spring (T_{2m}MAM), summer (T_{2m}JJA) and autumn (T_{2m}SON) 13 and 14: volumetric soil water in spring and (SoilWaterMAM) autumn (SoilWaterSON); 15 and 16: volumetric soil ice in winter and (SoilIceDJF) summer (SoilIceJJA). The abbreviations of the bio-climatic indicators are described in Section 3.2 and in Table 1. The spatial pattern of the averaged 1991–2023 scores for both components in every ecoregion, including their corresponding loadings, are shown in Fig. S5-S9.

315 According to the first (PC1) and second component (PC2) spatial maps (Fig. S5-S9), PC1 is found to be highly controlled by the topography of the ecoregion, and is consequently dependent on temperature (and through that on elevation), making GrowDays the bio-climatic indicator with the highest loading in all ecoregions, and therefore, the most significant contributor to the pattern represented by PC1. The PC2 is heavily shaped by continentality, permafrost extent and precipitation patterns, meaning that snow-related indicators, like SWE_{MAX} and MeltRate have the highest explanatory power.

https://doi.org/10.5194/egusphere-2024-2571
Preprint. Discussion started: 18 September 2024

These two principal components together largely capture and explain Greenness distribution, as seen by scores with high summer spectral greenness often clustered in one specific quadrant of the biplot. The wide range of conditions and locations of greenness could be related to different plant communities. As GrowDays is the most important loading (displayed by the longest loading vector) across ecoregions, and given its small load along PC2, GrowDays depends little on precipitation patterns. In ecoregion 2, the ecoregion with the widest East-West coverage, greenness appears to extend from coastal to inland regions and summer greenness seems to depend considerably on the snowpack of the preceding cold season (SWE_{MAX} loading vector opposite to Greenness loading vector). The decreasing trend of snow rates (SnowDJF and SnowMAM) has led to SWE_{MAX}DOY to occur earlier. Despite the increasing trend in T_{2m}MAM, the still-low solar elevation and the still-low near-surface air-temperatures result in low melting rates of the snowpack (MeltRate). These slow melt rates favour slow meltwater percolation (SoilWaterMAM loading vector opposite to MeltRate loading vector). Additionally, the earlier onset of the thermal growing season allows vegetation to produce energy via photosynthesis, particularly in the ecoregions in lower latitudes with adequate sun exposure (Onset loading vector opposite to Greenness loading vector). A wide atmospheric warming, that is assumed by the general increase in T_{2m}JJA in most ecoregions (Fig. S2), has resulted in increases of RainRatioJJA, despite the decrease of summer precipitation between 1991 and 2023 (Fig. S10). Therefore, increases of RainRatioJJA promote higher greenness (aligned loading vectors), as vegetation in such environmentally harsh places likely developed mechanisms to effectively retain/absorb liquid water whenever possible. Additionally, the increase in T_{2m}JJA generally favours less SoilIceJJA (opposed loading vectors). This is evident in the northern ecoregions, where summer rainfall has also increased, enhancing surface warming. The remaining ecoregions show localized increases in SoilWaterJJA, which is in contrast with significant decreases in ecoregion 2. We attribute the decrease in SoilWaterJJA to higher rates of evaporation in the more continental areas of ecoregion 2, supported by the significant increase in VPdJJA in the region. The energy necessary to convert liquid water into water vapour (latent heat) cools down the soil. Despite increase in T_{2m}JJA in ecoregion 2, the little change found in SoilIceJJA trends reinforces this hypothesis. The presence of vegetation canopy from dwarf shrubs, that helps to shade the ground in summer, could be an additional aspect to consider for the preservation of SoilIceJJA across permafrost areas in ecoregion 2. Also, the increased T_{2m}SON is in alignment with the increase in RainRatioSON and SoilWaterSON. This is of great relevance for vegetation growth in the southern ecoregions, where the end of the thermal growing season comes later.

We attempted to use the preceding autumn bio-climatic indicators to understand whether the start of the snow period could have played a role in the following growing season. However, the explained variance in PCA changed little (decreases of approx. 2-3% per ecoregion) and the relative importance of all loadings remained similar. Additionally, we correlated the interannual explained variance of the first two principal components with averaged climate oscillations (NAO and GBI) during the warm season (March to September), spring and summer. We noted that the interannual change in explained variance is not significantly correlated with seasonal climate oscillations.

4.3 Coastal, latitudinal and altitudinal dependence on trends

The significant increase in length of the thermal growing season (GrowDays) across ice-free Greenland is shown in Figure 5. An evident increase in the number of GrowDays occurs in Southwest Greenland at low-laying regions below 600 meters above

https://doi.org/10.5194/egusphere-2024-2571
Preprint. Discussion started: 18 September 2024

sea level (asl). At a local scale, significant increase is also found at elevations above 1000 m asl, more specifically within Nuup
355 Kangerlua (east of Nuuk) and Angujaartorfiup Nunaa (in between Maniitsoq Ice Cap and Kangerlussuaq). Such areas are in precipitation shadows, with reduced snow depths, but close to glaciers and ice caps. Along the narrow ice-free stripes in the Southeast, there is a modest increase of GrowDays (approx. 5 days per decade), at several elevations around Tasiilaq. The most pronounced increase in the number of GrowDays occurs along the coast facing the Denmark Strait.

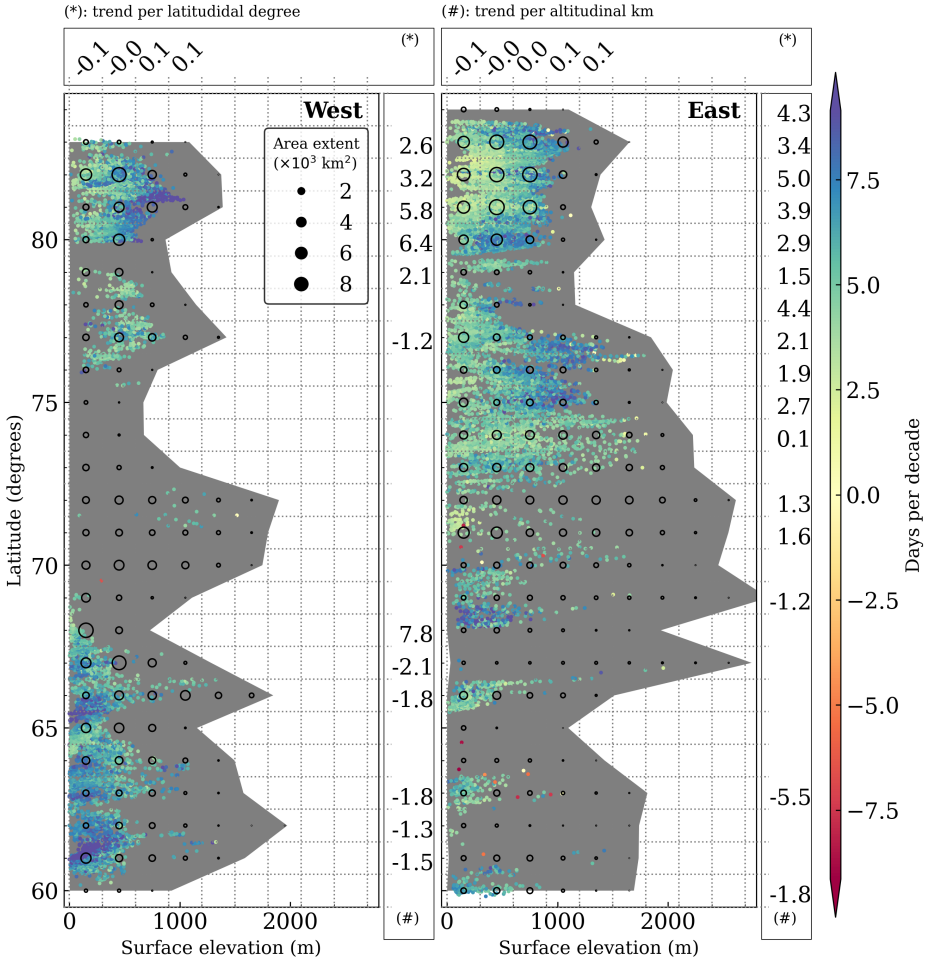

Figure 5. Significant trends for GrowDays (in days per decade) in the ice-free part of West (left panel) and East (right panel) Greenland. The trend's elevation dependency (in days per decade per altitudinal km) is binned in one degree of latitude and shown in vertical boxes marked with (#). The trend's latitudinal dependence (in days per decade per latitudinal degree) is binned every 300 m and shown in horizontal boxes marked with (*). The background grey shade displays the altitudinal extent of ice-free Greenland in the respective degree latitude, and the black circles represent the area extent by altitudinal and latitudinal bin. At least 50 pixels (approx. 312 km^2) are required within each bin to compute its regression, otherwise not displayed. Trends are considered significant for confidence levels in the Mann-Kendall trend test higher than 90%.

https://doi.org/10.5194/egusphere-2024-2571
Preprint. Discussion started: 18 September 2024

The vast and relatively flat ice-free Jameson Land (east of Ittoqqortoormiit, between 70° and 72°N), shows little evidence of GrowDays change within the past three decades. At the northernmost part of ecoregion 5 (75°N), areas at low elevations reveal the smallest increase of GrowDays in the ecoregion. This feature becomes even more pronounced in Greenland's northernmost regions, exhibiting the highest GrowDays elevation sensitivity (approx. 5 days per decade per km elevation), which is a contrasting elevation dependence in comparison with Southern Greenland. This tendency is modestly evident for the latitudinal sensitivity, mainly driven by high latitude and elevation trends: whereas GrowDays trends decrease with latitude in low-laying areas (< 300 m asl), GrowDays trends increase with latitude at higher elevations across North Greenland.

Trends for the onset of the thermal growing season resemble the trends in GrowDays, with earlier starts (approx. 8 days per decade) in southwest coastal Greenland and in the interior of Northeast Greenland. This comes as a consequence of shallower snow depths, that in combination with warming, has promoted longer snow-free periods. Thus, some areas of these ecoregions show increased trends in the number of frost days in spring. The thermal growing season trends along ice-free Greenland (Fig. 5) reveal prolonged periods of snow-free conditions, allowing certain vegetation communities to grow and expand. However, the increase in length of the thermal growing season is only one of several contributors to spectral greenness.

4.4 Greenness expansion and greening

Trends in summer spectral greenness are shown in Figure 6a. Significant greening occurs throughout Greenland, with pronounced greening across all ecoregions. Marked greening in ecoregion 1 is found in East Disko and northeast of Disko Bay. In ecoregion 2, the most pronounced greening is along the inland part of the Kangerlussuaq Fjord. The interior of Nuup Kangerlua evidence the highest greening in ecoregion 3. The coastal Kujalleq municipality, facing Labrador Sea, exhibits substantial greening. There are two greening clusters in ecoregion 5, being Jameson Land in the south, and the interior of King Christian X Land, in the north. In contrast, decreases in summer greenness are shown along the Southwest coast from ecoregion 1 to ecoregion 3, and in the interior of ecoregion 2.

In order to assess which regions became greener due to spectral vegetation expansion, we annually detected whether a pixel meets the spectral greenness criterion from 1991 to 2023. Then, we evenly split the study period into two and counted the total number of summers with spectral greenness within the two sub-periods. The result (Fig. 6c) shows the number of summers that are spectrally green in the second sub-period (2008-2023) with respect to the first sub-period (1991-2007), hereafter called changes in greenness distribution. The map of changes in greenness distribution shows that a considerable part of summer trends in spectral greening result from an expansion of vegetation. With the support of such a map, we discern that the relationship between changes in spectral greenness and its distribution are not linear. For instance, the central part of ecoregion 2 had as many summers of greenness in the second half as it had in the first half of the study period. Therefore, the changes in spectral greenness are either related to greening density of the existing vegetation or plant community change in ecoregion 2. The increased trend in spectral greenness of the remaining areas seems to be the result of spectral greenness expansion, likely due to the colonization of previously bare ground. The decreased trend in spectral greenness along the coastal southwest suggests that spectral vegetation is not as dense in the second sub-period as it used to be. Also, vegetation seems to be emerging directly adjacent to the ice-sheet.

https://doi.org/10.5194/egusphere-2024-2571
Preprint. Discussion started: 18 September 2024

Figure 6b combines the information of both maps by displaying significant changes in greenness as a function of latitude and latitude, colour-coded by the changes in greenness distribution. Ecoregions 3 and 4 show shrinkage in greenness at elevations lower than 500 m, while ecoregion 2 shows shrinkage up to 1000 m at certain latitudinal bands. In contrast, expansion in greenness is not only shifting upward but also northward across all ecoregions, with notorious upward advancements south of Kangerlussuaq towards Angujaartorfiup Nunaa in the west and in Jameson Land in the east.

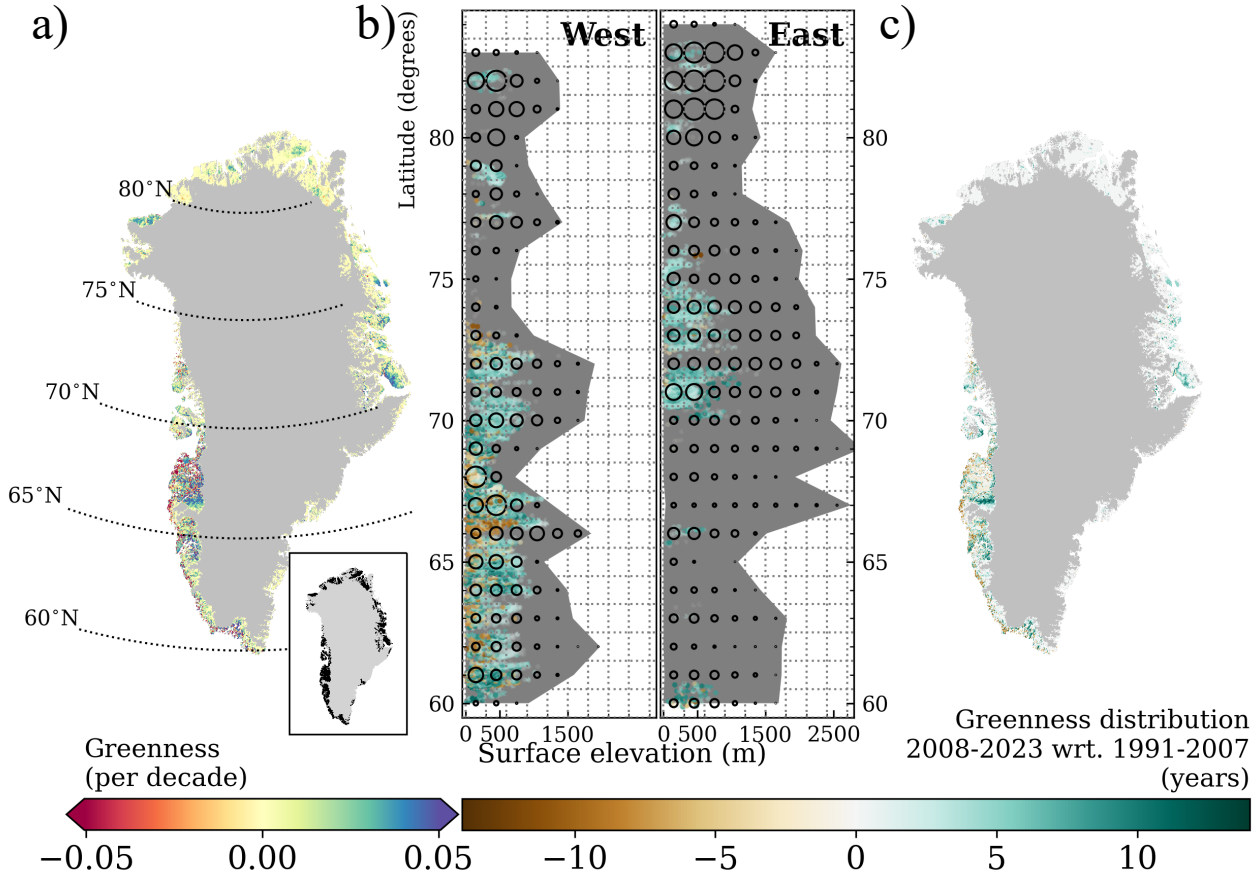

Figure 6. Trends in Greenness in Greenland (a). Significant trends are shown in the inset of (a) Trends are considered significant for confidence levels in the Mann-Kendall trend test higher than 90%. Difference in summer greenness for the period 2008-2023 with respect to (wrt.) the period 1991-2007, called as changes in greenness distribution (c). Changes in greenness distribution as a function of latitude and elevation at locations with significant trends in spectral greenness in West and East ice-free Greenland (b). The background grey shade displays the altitudinal extent of ice-free Greenland in the respective degree latitude, and the black circles qualitatively represent the area extent by altitudinal and latitudinal bin.

According to Table 2, we show that ecoregion 2 experienced the highest greenness expansion at 44.2%, along with the highest greenness reduction at 33.4% between 2008-2023 compared to 1991-2007, resulting in an overall increase of 10.7%

https://doi.org/10.5194/egusphere-2024-2571
Preprint. Discussion started: 18 September 2024

in vegetation greenness. Ecoregion 1 saw the largest increase in vegetation greenness at 22.2%, with a greenness expansion of 30.6%. Ecoregion 5 had the lowest greenness reduction at 2.7% and an overall increase in vegetation greenness of 19.8%. Ecoregions 3 and 4 also experienced increases in vegetation greenness, at 18% and 20%, respectively.

Table 2. Percentage of vegetation expansion and shrinkage, and ratio (fraction of expansion by shrinkage) between 2008-2023 with respect to 1991-2007 in every ecoregion

	Ecoregion 1	Ecoregion 2	Ecoregion 3	Ecoregion 4	Ecoregion 5
Expansion	30.6	44.2	38.6	28.0	22.5
Shrinkage	8.4	33.4	20.5	7.9	2.7
Ratio	3.6	1.3	1.8	3.5	8.3

The southernmost and the northernmost ecoregions experience the highest expansion ratios, ranging from three times to eight times more expansion than shrinkage in Ecoregion 4 and 5, respectively. Overall, vegetation expansion in ice-free Greenland increases two times faster than vegetation reduction between 2008-2023 compared to 1991-2007.

5 Discussion

5.1 Key findings in the context of the current literature

For the first time, bio-climatic indicators driving spectral greenness were statistically aggregated to better understand their combined relevance across ice-free Greenland. This is achieved by using principal component analysis (PCA) on remote-sensing data of spectral greenness and the output of a polar-adapted reanalysis. We demonstrated that the first two principal components account for most of the variability among the 16 combined bio-climatic indicators. These indicators were chosen to be of relevance to the ecological processes of tundra ecosystems. Given the fact that the chosen indicators are interlinked with supplementary indicators, we extended the interpretation to over 30 bio-climatic factors.

PCA effectively clustered bio-climatic indicators that co-vary with summer spectral greenness. Numerous indicators are closely correlated with air-temperature and topography (PC1), and less on precipitation patterns (PC2), except for ecoregion 2. The rank of relative importance of individual bio-climatic indicators depends on ecoregion, with the number of days of the thermal growing season (GrowDays) being the most relevant across all ecoregions. Our results suggest that in the northern ecoregions, the reduction in soil ice during summer (SoilIceJJA), due to warm and wet summers, is enabling vegetation growth, leading to northward expansion of vegetation. This reduction in SoilIceJJA is accompanied by substantial increases in air-temperature (T_{2m}JJA) and the fraction of liquid precipitation (RainRatioJJA) during summer. However, due to the low precipitation rates at high latitudes, permafrost thawing is suggested as an important source of soil water availability. Regions with significant decreases in maximum snow water equivalent (SWE_{MAX}) evidence early SWE_{MAX} day of the year (DOY) that leads to early onset of the GrowDays across ecoregions. Northwest Greenland, including ecoregion 1 is the only exception, where wide-spread increases in SWE_{MAX} along coastal areas has led to delays of the onset of the GrowDays. Despite increased

https://doi.org/10.5194/egusphere-2024-2571
Preprint. Discussion started: 18 September 2024

amounts of fresh snow and fewer drought days in spring in Southwest Greenland, the decreasing trend in SWE_{MAX} in ecoregions 3 and 4 is attributed to reduced winter snowfall. In most ecoregions, we find that shallower snowpacks melt at lower rates than deep snow. This has been mentioned in literature and is attributed to global warming. Musselman et al. (2017) explains that in Western North America this is a consequence of the snow season contraction. Warmer near-surface temperatures in spring trigger and sustain slow snowmelt rates, as shallow snow depths require less energy to initiate snowmelt. In contrast, deep snowpacks that require more energy to initiate melt, are more likely to refreeze snowmelt water within the snowpack (Dingman, 2015). Therefore, slow snowmelt rates in shallow snowpacks allow for efficient soil water absorption (Stephenson and Freeze, 1974), eventually used by microbial activity for decomposition of soil organic matter and then releasing soil nutrients (Heijmans et al., 2022). The combined effect of soil nutrients with increased soil water availability in spring (SoilWaterMAM) and T_{2m}MAM, promotes early plant growth. Therefore, leaves are more developed in early summer, which in association with increased T_{2m}JJA and longer periods of solar radiation, allow for greener vegetation.

The drier conditions in the interior of ecoregion 2 have led to losses in volumetric soil water during summer (SoilWaterJJA) with minimal changes in SoilIceJJA. This forces and limits vegetation distribution towards the proximity of water bodies. Additionally, despite decreases in SoilWaterJJA in ecoregion 2, our results showed increased trends in spring and autumn as a result of slow snowmelt and increased rain ratio, respectively. Grimes et al. (2024) investigated land cover changes across Greenland by using Landsat images since the late 1980s and found similar spatial patterns of vegetation change. For instance, they showed increases in coverage of vegetation southwest of Kangerlussuaq. They attributed this increase of vegetation to receding lakes happening, at least, since 1995 (Law et al., 2018). Similar to our findings, Grimes et al. (2024) detected increased vegetation cover in northeast of Kangerlussuaq. This has been shown and modelled in other parts of the Arctic tundra (e.g., Bosson et al. 2023; Jones and Henry 2003). Specifically, in ecoregion 2 and 5, vegetation is not only expanding inland, but also upward. The interior of Greenland, less exposed to frontal systems developing over the Atlantic and with meltwater availability, seems to be favourable areas for vegetation growth. Although there are no significant trends in SWE_{MAX} in ecoregion 2, subsurface runoff from permafrost thaw and meltwater from nearby snow/ice bodies likely contribute to the increase in SoilWaterMAM in the area. Episodic rainfall events in spring can also contribute to increased SoilWaterMAM. However, no significant changes in accumulated rain nor in rain ratio in spring (RainRatioMAM) were found in the region. According to Grimes et al. (2024), the retreat of vegetation in front of the Maniitsoq Ice Cap is leading to the exposure of bedrock. Additionally, the less dense summer vegetation in coastal ecoregion 2 and along ecoregion 3 is suggested by Grimes et al. (2024) to be related to the increase in freshwater, likely due to increased river discharge. A small-scale study, north of Kangerlussuaq, reports declining growth of deciduous shrubs (Gamm et al., 2018) since the 1990s. A similar signal is seen regionally in our results. They reported that the decrease is likely due to water soil scarcity, being a markedly pronounced negative trend for SoilWaterJJA in the region. The derived spatio-temporal patterns of summer precipitation (Fig. S10) and rain ratio are also in agreement with literature (e.g., Huai et al. 2022; van der Schot et al. 2023), especially on the significant increase of the rain ratio in North and West Greenland in summer and autumn. This consistency with other studies demonstrates the potential of the Copernicus Arctic regional reanalysis (CARRA) for biogeographic studies.

https://doi.org/10.5194/egusphere-2024-2571
Preprint. Discussion started: 18 September 2024

We report little to no change in the length and onset of the GrowDays along the coast in Northeast Greenland. In situ long-term measurements (e.g., Schmidt et al. 2023), state that some taxa may have reached their phenological limits despite ongoing warming. Assmann et al. (2019) suggests that temperature and snowmelt explain the effects on spring phenology in Zackenberg, contrary to sea-ice break up in the Greenland Sea. However, the continuous southward transport of cold waters, frequently with sea ice, through the East Greenland current likely stabilizes the onset of the GrowDays at the coast. This effect is dampened towards the interior and high elevations in Northeast Greenland, resulting in elevation sensitivity.

The wide-spread summer spectral greening occurs as a result of greener vegetation at certain sites. This likely occurred due to encroachment of vegetation on previously bare surfaces and changes in plant community composition. Spectral greenness correlates best with biophysical properties, such as leaf area index (Myers-Smith et al., 2020). Therefore, we may argue that the spectral greening is generally related to tundra shrub expansion throughout the past three decades, as early proposed by Sturm et al. (2001).

5.2 Implications

Longer thermal growing seasons are shown across Greenland between 1991 and 2023. Longer thermal growing seasons, associated with higher air-temperatures, favour vegetation growth. However, further investigation is required to comprehend the impacts on vegetation and ecosystem functioning in regions that may face severe freezing conditions in the future due to reduced snow cover and changing precipitation patterns. Since our study determines a set of bio-climatic indicators relevant for spectral greenness, such insights can now be used to validate the same bio-climatic indicators retrieved from the historical period of global climate models to assess future vegetation changes across Greenland under a changing climate.

The terrestrial Arctic biosphere is an important regional source of primary biological aerosol particles (PBAPs), highly correlated with air-temperature and surface vegetation. These aerosol particles were found to play an important role in cloud formation, specifically in the Arctic with low aerosol concentrations (e.g., Pereira Freitas et al. 2023; Sze et al. 2022). Therefore, the increased air-temperature and changes in vegetation can significantly impact cloud properties, such as cloud phase, radiative properties, cloud lifetime, and precipitation patterns, which in turn impact the surface conditions. Such PBAPs can be advected towards snow- and ice-covered regions, for instance the Greenland ice sheet, contributing to the surface darkening and enhancing algae growth (Feng et al. 2024) which again leads to increased melt, particularly of the ice bodies in the vicinity of densely vegetated regions.

With decreasing sea ice, fog conditions are very likely to become more frequent in certain coastal parts of Greenland (Song et al., 2023). Water droplets from fog can effectively be retained by tundra vegetation and are not accounted as a water source. This interaction between fog, vegetation and soil should be better investigated in tundra vegetation.

Longer thermal growing season could have also significant large-scale implications for biodiversity. Prolonged warmth may foster the proliferation of shrubs, leading to increased "shrubification" and potentially resulting in the homogenization of species compositions across these landscapes (Myers-Smith et al., 2011). This ecological shift might will also affect animal communities such as birds (Boelman et al., 2015) and arthropods (Høye et al., 2018). Ultimately, the increased growing season

https://doi.org/10.5194/egusphere-2024-2571
Preprint. Discussion started: 18 September 2024

could create favourable conditions for invasive species to establish and spread, further threatening the native biodiversity and altering the delicate balance of these unique environments (e.g., Elmendorf et al. 2012; Pearson et al. 2013).

5.3 Study limitations

There are limitations in the use of NDVI for the characterization of changes in plant communities (e.g., Myers-Smith et al. 2020). This includes that NDVI is good at capturing plant communities with a high composition of shrubs (e.g., Blok et al. 2011), but it is not as good at detecting communities with low infrared reflectance or sparsely vegetated areas. Our methods in combination with proposed approaches as Karami et al. (2018) and Rudd et al. (2021), who categorized tundra vegetation classes across ice-free Greenland, would allow an optimal assessment of spatio-temporal changes among plant communities. However, the high spatial resolution of optical satellite images from Landsat 8 and Sentinel 2 are only collected for approximately a decade. Another limitation regarding the NDVI analysis is that pixels associated with certain vegetation types (e.g., wet tundra) may be misinterpreted by adjacent water bodies, likely influencing spectral vegetation extent and trend magnitudes of certain areas, such as shown in ecoregion 2. Additionally, certain low-lying strips near fjords are very narrow, potentially causing errors in pixel reflectance calculations due to limited spatial resolution. Remote-sense NDVI products highly depends on the weather conditions in order to retrieve surface reflectance. Occasions with snow, shadows and clouds are thus assumed to be evenly distributed through time. Also, spectral greenness highly responds to the prevailing atmospheric circulation patterns. An exceptional period in frequency and intensity of anti-cyclonic activity between 2010 and 2019, promoted advection of relatively warm and humid air from the North Atlantic towards Southwest Greenland (Silva et al., 2022). Such periods have favoured exceptional vegetation growth across western ecoregions. Despite the frequency of prevailing atmospheric circulation patterns, there is a superimposed warming signal, with less cold conditions promoting vegetation growth.

Even though CARRA is able to capture spatio-temporal changes on relevant bio-climatic indicators influencing spectral greenness, the effect of shrub canopies on the ground conditions are likely not captured. This implies that potential feedback loops (e.g., Hallinger et al. 2010; Barrere et al. 2018), where shrub growth and expansion result in more snow trapping during winter, thereby enhancing winter soil insulation, increased microbial activity, and more soil organic matter in spring, along with greater shading in the following summer (Blok et al., 2010) cannot be assessed yet. Additionally, the vegetation type was recently considered as a strong predictor of summer surface turbulent fluxes, latent and sensible heat fluxes (Oehri et al., 2022). Such mechanisms must be acknowledged for future projections of vegetation change in the Arctic. Also, the representativeness of the permafrost extent and active layer thickness will be key aspects to consider, as permafrost areas are rich in soil moisture and nutrients. Thus, areas under permafrost thawing are likely spots for future vegetation expansion, especially if the current trend in decreased summer precipitation remains. For the next decades, melting of glaciers and ice caps will also provide sediments and nutrients through increased runoff.

Soil nutrients are also highly influenced by topography (not only elevation, but also relief and aspect), reflected in vegetation. According to Anderson (2020), organic rich soils in Greenland generally accumulate on north facing slopes, with little to none on the south facing slopes as a result of precipitation patterns, whereas in valley bottoms and at slope breaks, thicker fen-like, organic rich deposits accumulate. Even though we have investigated how vegetation and bio-climatic indicators are changing

https://doi.org/10.5194/egusphere-2024-2571
Preprint. Discussion started: 18 September 2024

as a function of latitude and elevation, potential influences due to relief and aspect should be considered, particularly at the local scale.

Our results show that summer spectral greenness appears statistically unresponsive to changes in rain on snow days (RainOnSnow) and below zero temperatures (FrostDays) during spring. Future work could rather focus on the analysis of extreme events and their impacts on greenness.

6 Conclusions

Our study aimed to better understand the long-term, large-scale interactions among various bio-climatic indicators and their collective effects on summer spectral greenness in ice-free Greenland. Bio-climatic changes are influenced by a complex set of factors, not only centred in summer, but also dependent on winter and spring atmospheric temperatures, precipitation, solar radiation, soil properties, and soil water availability. Using an unsupervised method like principal component analysis, we successfully represented and described the relationship between bio-climatic indicators and summer greenness in accordance with both small- and large-scale observational studies. This analysis utilized remote sensing Normalized Difference Vegetation Index and bio-climatic indicators from the Copernicus Arctic regional reanalysis between 1991 and 2023. For this period, we identified a set of bio-climatic indicators that co-vary with summer spectral greenness across ecoregions. While the relative importance for most of these indicators is similar in different ecoregions, their spatio-temporal changes depend on ecoregion, elevation and latitude. Overall, the bio-climatic changes during the study period led to more vegetation expansion, particularly towards the interior and northward, rather than vegetation reduction.

Data availability. The Normalized Difference Vegetation Index CDR used in this study was acquired from NOAA's National Centers for Environmental Information (http://www.ncei.noaa.govhttp://www.ncei.noaa.gov). This CDR was originally developed by Eric Vermote and colleagues for NOAA's CDR Program.

Schyberg et al. (2020) was downloaded from the Copernicus Climate Change Service (2024). The results contain modified Copernicus Climate Change Service information 2024. Neither the European Commission nor ECMWF is responsible for any use that may be made of the Copernicus information or data it contains.

The North Atlantic Oscillation and Greenland Blocking Index data were obtained from the NCEP/CPC and the PSL/ESRL, respectively. Both climate oscillations were seasonally standardized relative to the period 1950-2000.

Author contributions. The inspiration for the paper was brought by BSW, EMB, IGA, JA and NdV, the concept and methodology was developed by TS, the original paper draft was written by TS, the data were processed and analyzed by TS, all authors contributed to the interpretation of results as well as reviewing and editing the final paper draft.

https://doi.org/10.5194/egusphere-2024-2571
Preprint. Discussion started: 18 September 2024

Competing interests. The authors declare that they have no conflict of interest.

555 *Acknowledgements.* The University of Graz is acknowledged for support of publication costs. Brandon S. Whitley, Elisabeth M. Biersma and Natasha de Vere have received funding from the Carlsberg Foundation. The main author would like to acknowledge the use of OpenAI's ChatGPT for assisting in the writing and editing of this manuscript. The chatbot was utilized to enhance the clarity and readability of the text. A special thanks to Inger Greve Alsos and Therese Rieckh for their valuable suggestions.

https://doi.org/10.5194/egusphere-2024-2571
Preprint. Discussion started: 18 September 2024

References

Aalto, J., Lehtonen, I., Pirinen, P., Aapala, K., and Heikkinen, R. K.: Bioclimate change across the protected area network of Finland, Science of the Total Environment, 893, 164 782, https://doi.org/10.1016/j.scitotenv.2023.164782, 2023.

Abermann, J., Van As, D., Wacker, S., Langley, K., Machguth, H., and Fausto, R. S.: Strong contrast in mass and energy balance between a coastal mountain glacier and the Greenland ice sheet, Journal of Glaciology, 65, 263–269, https://doi.org/10.1017/jog.2019.4, 2019.

Ackerman, D., Griffin, D., Hobbie, S. E., and Finlay, J. C.: Arctic shrub growth trajectories differ across soil moisture levels, Global Change Biology, 23, 4294–4302, https://doi.org/10.1111/gcb.13677, 2017.

Anderson, N. J.: Terrestrial ecosystems of West Greenland, Encyclopedia of the World's Biomes, 1, 465–479, https://doi.org/10.1016/B978-0-12-409548-9.12486-8, 2020.

Assmann, J. J., Myers-Smith, I. H., Phillimore, A. B., Bjorkman, A. D., Ennos, R. E., Prevéy, J. S., Henry, G. H., Schmidt, N. M., and Hollister, R. D.: Local snow melt and temperature—but not regional sea ice—explain variation in spring phenology in coastal Arctic tundra, Global Change Biology, 25, 2258–2274, https://doi.org/https://doi.org/10.1111/gcb.14639, 2019.

Barrere, M., Domine, F., Belke-Brea, M., and Sarrazin, D.: Snowmelt events in autumn can reduce or cancel the soil warming effect of snow–vegetation interactions in the Arctic, Journal of Climate, 31, 9507–9518, https://doi.org/10.1175/JCLI-D-18-0135.1, 2018.

Bengtsson, L., Andrae, U., Aspelien, T., Batrak, Y., Calvo, J., de Rooy, W., Gleeson, E., Hansen-Sass, B., Homleid, M., Hortal, M., Ivarsson, K.-I., Lenderink, G., Niemelä, S., Nielsen, K. P., Onvlee, J., Rontu, L., Samuelsson, P., Muñoz, D. S., Subias, A., Tijm, S., Toll, V., Yang, X., and Køltzow, M. Ø.: The HARMONIE–AROME model configuration in the ALADIN–HIRLAM NWP system, Monthly Weather Review, 145, 1919–1935, https://doi.org/10.1175/MWR-D-16-0417.1, 2017.

Bjørk, A., Aagaard, S., Lütt, A., Khan, S., Box, J., Kjeldsen, K., Larsen, N., Korsgaard, N., Cappelen, J., Colgan, W., Machguth, H., Andresen, C. S., Y, P., and H, K. K.: Changes in Greenland's peripheral glaciers linked to the North Atlantic Oscillation, Nature Climate Change, 8, 48–52, https://doi.org/10.1038/s41558-017-0029-1, 2018.

Bliss, L. C., Courtin, G., Pattie, D., Riewe, R., Whitfield, D., and Widden, P.: Arctic tundra ecosystems, Annual Review of Ecology and Systematics, pp. 359–399, 1973.

Blok, D., Heijmans, M. M., Schaepman-Strub, G., Kononov, A., Maximov, T., and Berendse, F.: Shrub expansion may reduce summer permafrost thaw in Siberian tundra, Global Change Biology, 16, 1296–1305, https://doi.org/10.1111/j.1365-2486.2009.02110.x, 2010.

Blok, D., Schaepman-Strub, G., Bartholomeus, H., Heijmans, M. M., Maximov, T. C., and Berendse, F.: The response of Arctic vegetation to the summer climate: relation between shrub cover, NDVI, surface albedo and temperature, Environmental Research Letters, 6, 035 502, https://doi.org/10.1088/1748-9326/6/3/035502, 2011.

Boelman, N. T., Gough, L., Wingfield, J., Goetz, S., Asmus, A., Chmura, H. E., Krause, J. S., Perez, J. H., Sweet, S. K., and Guay, K. C.: Greater shrub dominance alters breeding habitat and food resources for migratory songbirds in Alaskan arctic tundra, Global Change Biology, 21, 1508–1520, https://doi.org/10.1111/gcb.12761, 2015.

Boertmann, D., Olsen, K., and Nielsen, R. D.: Geese in Northeast and North Greenland as recorded on aerial surveys in 2008 and 2009, Dansk Ornitologisk Forenings Tidsskrift, 109, 206–17, 2015.

Bosson, J.-B., Huss, M., Cauvy-Fraunié, S., Clément, J.-C., Costes, G., Fischer, M., Poulenard, J., and Arthaud, F.: Future emergence of new ecosystems caused by glacial retreat, Nature, 620, 562–569, https://doi.org/10.1038/s41586-023-06302-2, 2023.

Chen, Y., Cheng, X., Liu, A., Chen, Q., and Wang, C.: Tracking lake drainage events and drained lake basin vegetation dynamics across the Arctic, Nature Communications, 14, 7359, https://doi.org/10.1038/s41467-023-43207-0, 2023.

https://doi.org/10.5194/egusphere-2024-2571
Preprint. Discussion started: 18 September 2024

Cooper, E. J.: Warmer shorter winters disrupt Arctic terrestrial ecosystems, Annual Review of Ecology, Evolution, and Systematics, 45, 271–295, https://doi.org/10.1146/annurev-ecolsys-120213-091620, 2014.

Dingman, S. L.: Physical Hydrology, Waveland press, 2015.

Eikelenboom, M., Higgins, R. C., John, C., Kerby, J., Forchhammer, M. C., and Post, E.: Contrasting dynamical responses of sympatric caribou and muskoxen to winter weather and earlier spring green-up in the Arctic, Food Webs, 27, e00 196, https://doi.org/10.1016/j.fooweb.2021.e00196, 2021.

Elmendorf, S. C., Henry, G. H., Hollister, R. D., Björk, R. G., Boulanger-Lapointe, N., Cooper, E. J., Cornelissen, J. H., Day, T. A., Dorrepaal, E., Elumeeva, T. G., Gill, M., Gould, W. A., Harte, J., Hik, D. S., Hofgaard, A., Johnson, D. R., Johnstone, J. F., Jónsdóttir, I. S., Jorgenson, J. C., Klanderud, K., Klein, J. A., Koh, S., Kudo, G., Lara, M., Lévesque, E., Magnússon, B., May, J. L., Mercado-Díaz, J. A., Michelsen, A., Molau, U., Myers-Smith, I. H., Oberbauer, S. F., Onipchenko, V. G., Rixen, C., Schmidt, N. M., Shaver, G. R., Spasojevic, M. J., Þórhallsdóttir, t. E., Tolvanen, A., Troxler, T., Tweedie, C. E., Villareal, S., Wahren, C.-H., Walker, X., Webber, P. J., Welker, J. M., and Wipf, S.: Plot-scale evidence of tundra vegetation change and links to recent summer warming, Nature Climate Change, 2, 453–457, https://doi.org/10.1038/nclimate1465, 2012.

Ettema, J., Van den Broeke, M., Van Meijgaard, E., and Van de Berg, W.: Climate of the Greenland ice sheet using a high-resolution climate model–Part 2: Near-surface climate and energy balance, The Cryosphere, 4, 529–544, https://doi.org/10.5194/tc-4-529-2010, 2010.

Eythorsson, D., Gardarsson, S. M., Ahmad, S. K., Hossain, F., and Nijssen, B.: Arctic climate and snow cover trends–Comparing Global Circulation Models with remote sensing observations, International Journal of Applied Earth Observation and Geoinformation, 80, 71–81, https://doi.org/10.1016/j.jag.2019.04.003, 2019.

Feng, S., Cook, J. M., Naegeli, K., Anesio, A. M., Benning, L. G., and Tranter, M.: The Impact of Bare Ice Duration and Geo-Topographical Factors on the Darkening of the Greenland Ice Sheet, Geophysical Research Letters, 51, e2023GL104 894, https://doi.org/10.1029/2023GL104894, 2024.

Fettweis, X., Box, J. E., Agosta, C., Amory, C., Kittel, C., Lang, C., van As, D., Machguth, H., and Gallée, H.: Reconstructions of the 1900–2015 Greenland ice sheet surface mass balance using the regional climate MAR model, The Cryosphere, 11, 1015–1033, https://doi.org/10.5194/tc-11-1015-2017, 2017.

Franch, B., Vermote, E. F., Roger, J.-C., Murphy, E., Becker-Reshef, I., Justice, C., Claverie, M., Nagol, J., Csiszar, I., Meyer, D., Baret, F., Masuoka, E., Wolfe, R., and Devadiga, S.: A 30+ year AVHRR land surface reflectance climate data record and its application to wheat yield monitoring, Remote Sensing, 9, 296, https://doi.org/10.3390/rs9030296, 2017.

Gamm, C. M., Sullivan, P. F., Buchwal, A., Dial, R. J., Young, A. B., Watts, D. A., Cahoon, S. M., Welker, J. M., and Post, E.: Declining growth of deciduous shrubs in the warming climate of continental western Greenland, Journal of Ecology, 106, 640–654, https://doi.org/10.1111/1365-2745.12882, 2018.

Gilson, G. F., Jiskoot, H., Gueye, S., and van Boxel, J. H.: A climatology of Arctic fog along the coast of East Greenland, Quarterly Journal of the Royal Meteorological Society, 150, 706–726, 2024.

Grimes, M., Carrivick, J. L., Smith, M. W., and Comber, A. J.: Land cover changes across Greenland dominated by a doubling of vegetation in three decades, Scientific Reports, 14, 3120, https://doi.org/10.1038/s41598-024-52124-1, 2024.

Grossiord, C., Buckley, T. N., Cernusak, L. A., Novick, K. A., Poulter, B., Siegwolf, R. T., Sperry, J. S., and McDowell, N. G.: Plant responses to rising vapor pressure deficit, New phytologist, 226, 1550–1566, https://doi.org/10.1111/nph.16485, 2020.

Hallinger, M., Manthey, M., and Wilmking, M.: Establishing a missing link: warm summers and winter snow cover promote shrub expansion into alpine tundra in Scandinavia, New Phytologist, 186, 890–899, https://doi.org/10.1111/j.1469-8137.2010.03223.x, 2010.

https://doi.org/10.5194/egusphere-2024-2571
Preprint. Discussion started: 18 September 2024

Hanna, E., Jones, J. M., Cappelen, J., Mernild, S. H., Wood, L., Steffen, K., and Huybrechts, P.: The influence of North Atlantic atmospheric and oceanic forcing effects on 1900–2010 Greenland summer climate and ice melt/runoff, International Journal of Climatology, 33, 862–880, https://doi.org/10.1002/joc.3475, 2013.

Hanna, E., Cropper, T. E., Jones, P. D., Scaife, A. A., and Allan, R.: Recent seasonal asymmetric changes in the NAO (a marked summer decline and increased winter variability) and associated changes in the AO and Greenland Blocking Index, International Journal of Climatology, 35, 2540–2554, https://doi.org/10.1002/joc.4157, 2015.

Hanna, E., Cropper, T. E., Hall, R. J., and Cappelen, J.: Greenland Blocking Index 1851–2015: a regional climate change signal, International Journal of Climatology, 36, 4847–4861, https://doi.org/10.1002/joc.4673, 2016.

Heijmans, M. M., Magnússon, R. Í., Lara, M. J., Frost, G. V., Myers-Smith, I. H., van Huissteden, J., Jorgenson, M. T., Fedorov, A. N., Epstein, H. E., Lawrence, D. M., and Limpens, J.: Tundra vegetation change and impacts on permafrost, Nature Reviews Earth & Environment, 3, 68–84, https://doi.org/10.1038/s43017-021-00233-0, 2022.

Hersbach, H., Bell, B., Berrisford, P., Hirahara, S., Horányi, A., Muñoz-Sabater, J., Nicolas, J., Peubey, C., Radu, R., Schepers, D., Simmons, A., Soci, C., Abdalla, S., Abellan, X., Balsamo, G., Bechtold, P., Biavati, G., Bidlot, J., Bonavita, M., De Chiara, G., Dahlgren, P., Dee, D., Diamantakis, M., Dragani, R., Flemming, J., Forbes, R., Fuentes, M., Geer, A., Haimberger, L., Healy, S., Hogan, R. J., Hólm, E., Janisková, M., Keeley, S., Laloyaux, P., Lopez, P., Lupu, C., Radnoti, G., de Rosnay, P., Rozum, I., Vamborg, F., Villaume, S., and Thépaut, J.-N.: The ERA5 global reanalysis, Quarterly Journal of the Royal Meteorological Society, 146, 1999–2049, https://doi.org/10.1002/qj.3803, 2020.

Høye, T. T., Bowden, J. J., Hansen, O. L., Hansen, R. R., Henriksen, T. N., Niebuhr, A., and Skytte, M. G.: Elevation modulates how Arctic arthropod communities are structured along local environmental gradients, Polar Biology, 41, 1555–1565, https://doi.org/10.1007/s00300-017-2204-2, 2018.

Huai, B., van den Broeke, M. R., Reijmer, C. H., and Noël, B.: A daily 1-km resolution Greenland rainfall climatology (1958–2020) from statistical downscaling of a regional atmospheric climate model, Journal of Geophysical Research: Atmospheres, 127, e2022JD036 688, https://doi.org/10.1029/2022JD036688, 2022.

Huang, M., Piao, S., Janssens, I. A., Zhu, Z., Wang, T., Wu, D., Ciais, P., Myneni, R. B., Peaucelle, M., Peng, S., Yang, H., and Peñuelas, J.: Velocity of change in vegetation productivity over northern high latitudes, Nature Ecology & Evolution, 1, 1649–1654, 2017.

Hurrell, J. W., Kushnir, Y., Ottersen, G., and Visbeck, M.: An overview of the North Atlantic oscillation, Geophysical Monograph-American Geophysical Union, 134, 1–36, https://doi.org/10.1029/134GM01, 2003.

Hussain, M. and Mahmud, I.: pyMannKendall: a python package for non-parametric Mann Kendall family of trend tests., Journal of Open Source Software, 4, 1556, https://doi.org/10.21105/joss.01556, 2019.

Jansen, E., Christensen, J. H., Dokken, T., Nisancioglu, K. H., Vinther, B. M., Capron, E., Guo, C., Jensen, M. F., Langen, P. L., Pedersen, R. A., Yang, S., Bentsen, M., Kjær, H. A., Sadatzki, H., Sessford, E., and Stendel, M.: Past perspectives on the present era of abrupt Arctic climate change, Nature Climate Change, 10, 714–721, 2020.

Jones, G. A. and Henry, G. H.: Primary plant succession on recently deglaciated terrain in the Canadian High Arctic, Journal of Biogeography, 30, 277–296, https://doi.org/10.1046/j.1365-2699.2003.00818.x, 2003.

Karami, M., Hansen, B. U., Westergaard-Nielsen, A., Abermann, J., Lund, M., Schmidt, N. M., and Elberling, B.: Vegetation phenology gradients along the west and east coasts of Greenland from 2001 to 2015, Ambio, 46, 94–105, https://doi.org/10.1007/s13280-016-0866-6, 2017.

https://doi.org/10.5194/egusphere-2024-2571
Preprint. Discussion started: 18 September 2024

Karami, M., Westergaard-Nielsen, A., Normand, S., Treier, U. A., Elberling, B., and Hansen, B. U.: A phenology-based approach to the classification of Arctic tundra ecosystems in Greenland, ISPRS Journal of Photogrammetry and Remote Sensing, 146, 518–529, https://doi.org/10.1016/j.isprsjprs.2018.11.005, 2018.

Laird, N. F., Crossett, C. C., Keaton, G. A., and Hopson, L. N.: Weather conditions and seasonal variability of limited surface visibility at Greenland coastal locations, International Journal of Climatology, 44, 393–405, https://doi.org/10.1002/joc.8332, 2024.

Lamichhane, J. R.: Rising risks of late-spring frosts in a changing climate, Nature Climate Change, 11, 554–555, https://doi.org/10.1038/s41558-021-01090-x, 2021.

Law, A., Nobajas, A., and Sangonzalo, R.: Heterogeneous changes in the surface area of lakes in the Kangerlussuaq area of southwestern Greenland between 1995 and 2017, Arctic, Antarctic, and Alpine Research, 50, S100 027, https://doi.org/10.1080/15230430.2018.1487744, 2018.

Le Moullec, M., Sandal, L., Grøtan, V., Buchwal, A., and Hansen, B. B.: Climate synchronises shrub growth across a high-arctic archipelago: contrasting implications of summer and winter warming, Oikos, 129, 1012–1027, https://doi.org/10.1111/oik.07059, 2020.

Liu, Y., Wang, P., Elberling, B., and Westergaard-Nielsen, A.: Drivers of contemporary and future changes in Arctic seasonal transition dates for a tundra site in coastal Greenland, Global Change Biology, 30, e17 118, https://doi.org/10.1111/gcb.17118, 2024.

Masson, V., Champeaux, J.-L., Chauvin, F., Meriguet, C., and Lacaze, R.: A global database of land surface parameters at 1-km resolution in meteorological and climate models, Journal of Climate, 16, 1261–1282, https://doi.org/10.1175/1520-0442(2003)16<1261:AGDOLS>2.0.CO;2, 2003.

Metcalfe, D. B., Hermans, T. D., Ahlstrand, J., Becker, M., Berggren, M., Björk, R. G., Björkman, M. P., Blok, D., Chaudhary, N., Chisholm, C., Classen, A. T., Hasselquist, N. J., Jonsson, M., Kristensen, J. A., Kumordzi, B. B., Lee, H., Mayor, J. R., Prevéy, J., Pantazatou, K., Rousk, J., Sponseller, R. A., Sundqvist, M. K., Tang, J., Uddling, J., Wallin, G., Zhang, W., Ahlström, A., Tenenbaum, D. E., and Abdi, A. M.: Patchy field sampling biases understanding of climate change impacts across the Arctic, Nature Ecology & Evolution, 2, 1443–1448, https://doi.org/10.1038/s41559-018-0612-5, 2018.

Musselman, K. N., Clark, M. P., Liu, C., Ikeda, K., and Rasmussen, R.: Slower snowmelt in a warmer world, Nature Climate Change, 7, 214–219, https://doi.org/10.1038/nclimate3225, 2017.

Myers-Smith, I. H., Forbes, B. C., Wilmking, M., Hallinger, M., Lantz, T., Blok, D., Tape, K. D., Macias-Fauria, M., Sass-Klaassen, U., Lévesque, E., Boudreau, S., Ropars, P., Hermanutz, L., Trant, A., Collier, L. S., Weijers, S., Rozema, J., Rayback, S. A., Schmidt, N. M., Schaepman-Strub, G., Wipf, S., Rixen, C., Ménard, C. B., Venn, S., Goetz, S., Andreu-Hayles, L., Elmendorf, S., Ravolainen, V., Welker, V., Grogan, P., Epstein, H. E., and Hik, D. S.: Shrub expansion in tundra ecosystems: dynamics, impacts and research priorities, Environmental Research Letters, 6, 045 509, https://doi.org/10.1088/1748-9326/6/4/045509, 2011.

Myers-Smith, I. H., Kerby, J. T., Phoenix, G. K., Bjerke, J. W., Epstein, H. E., Assmann, J. J., John, C., Andreu-Hayles, L., Angers-Blondin, S., Beck, P. S., Berner, L. T., Bhatt, U. S., Bjorkman, A. D., Blok, D., Bryn, A., Christiansen, C. T., Cornelissen, J. H. C., Cunliffe, A. M., Elmendorf, S. C., Forbes, B. C., Goetz, S. J., Hollister, R. D., de Jong, R., Loranty, M. M., Macias-Fauria, M., Maseyk, K., Normand, S., Olofsson, J., Parker, T. C., Parmentier, F.-J. W., Post, E., Schaepman-Strub, G., Stordal, F., Sullivan, P. F., Thomas, H. J. D., Tømmervik, H., Treharne, R., Tweedie, C. E., Walker, D. A., Wilmking, M., and Wipf, S.: Complexity revealed in the greening of the Arctic, Nature Climate Change, 10, 106–117, https://doi.org/10.1038/s41558-019-0688-1, 2020.

Nachtergaele, F., van Velthuizen, H., Verelst, L., Batjes, N., Dijkshoorn, K., van Engelen, V., Fischer, G., Jones, A., and Montanarela, L.: The harmonized world soil database, in: Proceedings of the 19th World Congress of Soil Science, Soil Solutions for a Changing World, Brisbane, Australia, 1-6 August 2010, pp. 34–37, 2010.

https://doi.org/10.5194/egusphere-2024-2571
Preprint. Discussion started: 18 September 2024

Oehri, J., Schaepman-Strub, G., Kim, J.-S., Grysko, R., Kropp, H., Grünberg, I., Zemlianskii, V., Sonnentag, O., Euskirchen, E. S., Reji Chacko, M., Muscari, G., Blanken, P. D., Dean, J. F., di Sarra, A., Harding, R. J., Sobota, I., Kutzbach, L., Plekhanova, E., Riihelä, A., Boike, J., Miller, N. B., Beringer, J., López-Blanco, E., Stoy, P. C., Sullivan, R. C., Kejna, M., Parmentier, F.-J. W., Gamon, J. A., Mastepanov, M., Wille, C., Jackowicz-Korczynski, M., Karger, D. N., Quinton, W. L., Putkonen, J., van As, D., Christensen, T. R., Hakuba, M. Z., Stone, R. S., Metzger, S., Vandecrux, B., Frost, G. V., Wild, M., Hansen, B., Meloni, D., Domine, F., te Beest, M., Sachs, T., Kalhori, A., Rocha, A. V., Williamson, S. N., Morris, S., Atchley, A. L., Essery, R., Runkle, B. R. K., Holl, D., Riihimaki, L. D., Iwata, H., Schuur, E. A. G., Cox, C. J., Grachev, A. A., McFadden, J. P., Fausto, R. S., Göckede, M., Ueyama, M., Pirk, N., de Boer, G., Bret-Harte, M. S., Leppäranta, M., Steffen, K., Friborg, T., Ohmura, A., Edgar, C. W., Olofsson, J., and Chambers, S. D.: Vegetation type is an important predictor of the arctic summer land surface energy budget, Nature Communications, 13, 6379, https://doi.org/10.1038/s41467-022-34049-3, 2022.

Pearson, R. G., Phillips, S. J., Loranty, M. M., Beck, P. S., Damoulas, T., Knight, S. J., and Goetz, S. J.: Shifts in Arctic vegetation and associated feedbacks under climate change, Nature Climate Change, 3, 673–677, https://doi.org/10.1038/nclimate1858, 2013.

Pedregosa, F., Varoquaux, G., Gramfort, A., Michel, V., Thirion, B., Grisel, O., Blondel, M., Prettenhofer, P., Weiss, R., Dubourg, V., Vanderplas, J., Passos, A., Cournapeau, D., Brucher, M., Perrot, M., and Duchesnay, E.: Scikit-learn: Machine Learning in Python, Journal of Machine Learning Research, 12, 2825–2830, http://jmlr.org/papers/v12/pedregosa11a.html, 2011.

Pedron, S., Jespersen, R., Xu, X., Khazindar, Y., Welker, J., and Czimczik, C.: More snow accelerates legacy carbon emissions from Arctic permafrost, AGU Advances, 4, e2023AV000 942, https://doi.org/10.1029/2023AV000942, 2023.

Pereira Freitas, G., Adachi, K., Conen, F., Heslin-Rees, D., Krejci, R., Tobo, Y., Yttri, K. E., and Zieger, P.: Regionally sourced bioaerosols drive high-temperature ice nucleating particles in the Arctic, Nature Communications, 14, 5997, https://doi.org/10.1038/s41467-023-41696-7, 2023.

Post, E. and Pedersen, C.: Opposing plant community responses to warming with and without herbivores, Proceedings of the National Academy of Sciences, 105, 12 353–12 358, https://doi.org/10.1073/pnas.0802421105, 2008.

Power, C. C., Normand, S., von Arx, G., Elberling, B., Corcoran, D., Krog, A. B., Bouvin, N. K., Treier, U. A., Westergaard-Nielsen, A., Liu, Y., and L. Prendin, A.: No effect of snow on shrub xylem traits: Insights from a snow-manipulation experiment on Disko Island, Greenland, Science of The Total Environment, 916, 169 896, https://doi.org/10.1016/j.scitotenv.2024.169896, 2024.

Rantanen, M., Karpechko, A. Y., Lipponen, A., Nordling, K., Hyvärinen, O., Ruosteenoja, K., Vihma, T., and Laaksonen, A.: The Arctic has warmed nearly four times faster than the globe since 1979, Communications Earth & Environment, 3, 168, 2022.

Rantanen, M., Kämäräinen, M., Niittynen, P., Phoenix, G. K., Lenoir, J., Maclean, I., Luoto, M., and Aalto, J.: Bioclimatic atlas of the terrestrial Arctic, Scientific Data, 10, 40, https://doi.org/10.1038/s41597-023-01959-w, 2023.

Rawlins, M. A. and Karmalkar, A. V.: Regime shifts in Arctic terrestrial hydrology manifested from impacts of climate warming, The Cryosphere, 18, 1033–1052, https://doi.org/10.5194/tc-18-1033-2024, 2024.

Rudd, D. A., Karami, M., and Fensholt, R.: Towards high-resolution land-cover classification of Greenland: A case study covering Kobbefjord, Disko and Zackenberg, Remote Sensing, 13, 3559, https://doi.org/10.3390/rs13183559, 2021.

Schmidt, N. M., Pedersen, S. H., Mosbacher, J. B., and Hansen, L. H.: Long-term patterns of muskox (Ovibos moschatus) demographics in high arctic Greenland, Polar Biology, 38, 1667–1675, https://doi.org/10.1007/s00300-015-1733-9, 2015.

Schmidt, N. M., Reneerkens, J., Christensen, J. H., Olesen, M., and Roslin, T.: An ecosystem-wide reproductive failure with more snow in the Arctic, PLoS Biology, 17, e3000 392, https://doi.org/10.1371/journal.pbio.3000392, 2019.

https://doi.org/10.5194/egusphere-2024-2571
Preprint. Discussion started: 18 September 2024

Schmidt, N. M., Kankaanpää, T., Tiusanen, M., Reneerkens, J., Versluijs, T. S., Hansen, L. H., Hansen, J., Gerlich, H. S., Høye, T. T., Cirtwill, A. R., Zhemchuzhnikov, M. K., Peña-Aguilera, P., and Roslin, T.: Little directional change in the timing of Arctic spring phenology over the past 25 years, Current Biology, 33, 3244–3249, https://doi.org/10.1016/j.cub.2023.06.038, 2023.

Schyberg, H., Yang, X., Køltzow, M., Amstrup, B., Bakketun, m., Bazile, E., Bojarova, J., Box, J. E., Dahlgren, P., Hagelin, S., Homleid, M., Horányi, A., Høyer, J., Johansson, m., Killie, M., Körnich, H., Le Moigne, P., Lindskog, M., Manninen, T., Nielsen, E. P., Nielsen, K., Olsson, E., Palmason, B., Peralta, A. C., Randriamampianina, R., Samuelsson, P., Stappers, R., Støylen, E., Thorsteinsson, S., Valkonen, T., and Wang, Z.: Arctic regional reanalysis on single levels from 1991 to present. Copernicus Climate Change Service (C3S) Climate Data Store (CDS), https://doi.org/10.24381/cds.713858f6, accessed on 15-12-2022, 2020.

Shahi, S., Abermann, J., Silva, T., Langley, K., Larsen, S. H., Mastepanov, M., and Schöner, W.: The importance of regional sea-ice variability for the coastal climate and near-surface temperature gradients in Northeast Greenland, Weather and Climate Dynamics, 4, 747–771, https://doi.org/10.5194/wcd-4-747-2023, 2023.

Silva, T., Abermann, J., Noël, B., Shahi, S., van de Berg, W. J., and Schöner, W.: The impact of climate oscillations on the surface energy budget over the Greenland Ice Sheet in a changing climate, The Cryosphere, 16, 3375–3391, https://doi.org/10.5194/tc-16-3375-2022, 2022.

Skakun, S., Justice, C. O., Vermote, E., and Roger, J.-C.: Transitioning from MODIS to VIIRS: an analysis of inter-consistency of NDVI data sets for agricultural monitoring, International Journal of Remote Sensing, 39, 971–992, https://doi.org/10.1080/01431161.2017.1395970, 2018.

Søgaard, D. H., Lund-Hansen, L. C., López-Blanco, E., Schmidt, N. M., Winding, M. H. S., Sejr, M. K., Rysgaard, S., Sorrell, B. K., Christensen, T. R., Juul-Pedersen, T., Tank, J. L., and Riis, T.: Arctic coastal nutrient limitation linked to tundra greening, Nature Communications, 2023.

Song, S., Chen, Y., Chen, X., Chen, C., Li, K.-F., Tung, K.-K., Shao, Q., Liu, Y., Wang, X., Yi, L., and Zhao, J.: Adapting to a Foggy Future Along Trans-Arctic Shipping Routes, Geophysical Research Letters, 50, e2022GL102 395, https://doi.org/10.1029/2022GL102395, 2023.

Stengel, M., Stapelberg, S., Sus, O., Finkensieper, S., Würzler, B., Philipp, D., Hollmann, R., Poulsen, C., Christensen, M., and McGarragh, G.: Cloud_cci Advanced Very High Resolution Radiometer post meridiem (AVHRR-PM) dataset version 3: 35-year climatology of global cloud and radiation properties, Earth System Science Data, 12, 41–60, https://doi.org/10.5194/essd-12-41-2020, 2020.

Stephenson, G. R. and Freeze, R. A.: Mathematical simulation of subsurface flow contributions to snowmelt runoff, Reynolds Creek Watershed, Idaho, Water Resources Research, 10, 284–294, 1974.

Sturm, M., Racine, C., and Tape, K.: Increasing shrub abundance in the Arctic, Nature, 411, 546–547, https://doi.org/10.1038/35079180, 2001.

Sze, K. C. H., Wex, H., Hartmann, M., Skov, H., Massling, A., Villanueva, D., and Stratmann, F.: Ice Nucleating Particles in Northern Greenland: annual cycles, biological contribution and parameterizations, Atmospheric Chemistry and Physics Discussions, 23, 1–45, https://doi.org/10.5194/acp-23-4741-2023, 2022.

van der Schot, J., Abermann, J., Silva, T., Jensen, C. D., Noël, B., and Schöner, W.: Precipitation trends (1958–2021) on Ammassalik island, south-east Greenland, Frontiers in Earth Science, 10, 1085 499, https://doi.org/10.3389/feart.2022.1085499, 2023.

van der Schot, J., Abermann, J., Silva, T., Rasmussen, K., Winkler, M., Langley, K., and Schöner, W.: Seasonal snow cover indicators in coastal Greenland from in-situ observations, a climate model and reanalysis, The Cryosphere, 18, 1033–1052, https://doi.org/10.5194/egusphere-2024-1999, 2024.

https://doi.org/10.5194/egusphere-2024-2571
Preprint. Discussion started: 18 September 2024

Vermote, E., Justice, C., Csiszar, I., Eidenshink, J., Myneni, R., Baret, F., Masuoka, E., Wolfe, R., Claverie, M., and Program, N. C.: NOAA Climate Data Record (CDR) of Normalized Difference Vegetation Index (NDVI), Version 5, https://doi.org/10.7289/V5ZG6QH9, access date: 2022-05-06, 2018.

Vermote, E., Franch, B., Roger, J.-C., Murphy, E., Becker-Reshef, I., Justice, C., Claverie, M., Nagol, J., Csiszar, I., Meyer, D., Baret, F., Masuoka, E., Wolfe, R., Devadiga, S., Villaescusa, J., and Program, N. C.: NOAA Climate Data Record (CDR) of Surface Reflectance, Version 1, https://doi.org/10.25921/gakh-st76, access date: 2023-07-06, 2022.

Walker, D. A., Raynolds, M. K., Daniëls, F. J., Einarsson, E., Elvebakk, A., Gould, W. A., Katenin, A. E., Kholod, S. S., Markon, C. J., Melnikov, E. S., Moskalenko, N. G., Talbot, S. S., Yurtsev, B. A., and other members of the CAVM Team, T.: The circumpolar Arctic vegetation map, Journal of Vegetation Science, 16, 267–282, https://doi.org/10.1111/j.1654-1103.2005.tb02365.x, 2005.

Wang, X., Li, Z., Xiao, J., Zhu, G., Tan, J., Zhang, Y., Ge, Y., and Che, T.: Snow cover duration delays spring green-up in the northern hemisphere the most for grasslands, Agricultural and Forest Meteorology, 355, 110 130, https://doi.org/10.1016/j.agrformet.2024.110130, 2024.

Weijers, S.: Declining temperature and increasing moisture sensitivity of shrub growth in the Low-Arctic erect dwarf-shrub tundra of western Greenland, Ecology and Evolution, 12, e9419, https://doi.org/10.1002/ece3.9419, 2022.

Weijers, S., Buchwal, A., Blok, D., Löffler, J., and Elberling, B.: High Arctic summer warming tracked by increased Cassiope tetragona growth in the world's northernmost polar desert, Global Change Biology, 23, 5006–5020, https://doi.org/10.1111/gcb.13747, 2017.

Westergaard-Nielsen, A., Karami, M., Hansen, B. U., Westermann, S., and Elberling, B.: Contrasting temperature trends across the ice-free part of Greenland, Scientific Reports, 8, 1586, https://doi.org/10.1038/s41598-018-19992-w, 2018.

Westergaard-Nielsen, A., Hansen, B. U., Elberling, B., and Abermann, J.: Greenland Climates, Encyclopedia of the World's Biomes, 1, 465–479, https://doi.org/10.1016/B978-0-12-409548-9.11750-6, 2020.

Yang, W., Tan, B., Huang, D., Rautiainen, M., Shabanov, N. V., Wang, Y., Privette, J. L., Huemmrich, K. F., Fensholt, R., Sandholt, I., Weiss, M., Ahl, D., Gower, S., Nemani, R., Knyazikhin, Y., and Myneni, R.: MODIS leaf area index products: From validation to algorithm improvement, IEEE Transactions on Geoscience and Remote Sensing, 44, 1885–1898, https://doi.org/10.1109/TGRS.2006.871215, 2006.

Yuan, H., Dai, Y., Xiao, Z., Ji, D., and Shangguan, W.: Reprocessing the MODIS Leaf Area Index products for land surface and climate modelling, Remote Sensing of Environment, 115, 1171–1187, https://doi.org/10.1016/j.rse.2011.01.001, 2011.

Yuan, W., Zheng, Y., Piao, S., Ciais, P., Lombardozzi, D., Wang, Y., Ryu, Y., Chen, G., Dong, W., Hu, Z., Jain, A. K., Jiang, C., Kato, E., Li, S., Lienert, S., Liu, S., Nabel, J. E., Qin, Z., Quine, T., Sitch, S., Smith, W. K., Wang, F., Wu, C., Xiao, Z., and Yang, S.: Increased atmospheric vapor pressure deficit reduces global vegetation growth, Science advances, 5, eaax1396, https://doi.org/10.1126/sciadv.aax1396, 2019.

Zwolicki, A., Zmudczyńska-Skarbek, K., Wietrzyk-Pełka, P., and Convey, P.: High Arctic vegetation, Encyclopedia of the World's Biomes, 1, 465–479, https://doi.org/10.1016/B978-0-12-409548-9.11771-3, 2020.